REFERENCE

REFERENCES

[1] **Bureau of Policy and Strategy.** (2011, December 14). Retrieved October 30, 2008, from http://bps.ops.moph.go.th/Statistic/2.3.4-52.pdf

[2] **Bureau of Policy and Strategy.** (2011, December 14). Retrieved October 30, 2008, from http://bps.ops.moph.go.th/cancer1/cancer/Untitled(55).html#Topic58

[3] Henry, R.Y. and Mahony, D.O. (1999). Treatment of prostate cancer. **Journal of Clinical Pharmacy and Therapeutics**, 24, 93-102

[4] Wiwanotkit, V. (2004). Prostate specific antigen for screening for prostate cancer: an appraisal of Thai reports. **Asian Pacific Journal of Cancer Prevention**, 5, 406-408.

[5] Buhachat, R. (2007). Current status of ovarian cancer. **Songklanagarind Medical Journal**, 25(6), 537-547.

[6] Yin, B.W.T, Dnistrian, A. and Lloyd, K.O. (2002). Ovarin cancer antigen CA125 is encoded by the *MUC16* MUCIN gene. **International Against Cancer**, 98, 737-740

[7] Yin, B.W.T, and Lloyd, K.O. (2001). Molecular cloning of the CA125 ovarin cancer antigen. **Journal of Biological Chemistry**, 276, 27371-27375.

[8] Thompson, I.M., Pauler, D.K., Goodman, P.J. Tangen, C.M., Lucia, M.S., Parnes, H.L., et al. (2004). Prevalence of Prostate Cancer among Men with a Prostate-Specific Antigen Level ≤4.0 ng per Milliliter. **The New England Journal of Medicine**, 350(22), 2239-2246.

[9] Jarukumjorn, K. and Chatuphonprasert, W. (2007). SNP: Basic knowledge to applications. **Thai Pharmaceutical and Health Science Journal**, 2(2), 166-174.

[10] Nielsen, P. E. (2001). Peptide nucleic acid: a versatile tool in genetic diagnostics and molecular biology. **Current Opinion in Biotechnology**, 12, 16-20.

[11] Griffin, T. J. and Smith, L. M. (2000). Single-nucleotide polymorphism analysis by MALDI-TOF mass spectrometry. **Trends in Biotechnology**, 18, 77-84.

[12] Renault, N.J., Martelet, C., Chevolot, Y. and Cloaree, J.P. (2007). Biosensor and bio-Bar code assays based on biofunctionalized magnetic microbeads. **Sensor,** 7, 589-614

[13] Murphy, L. (2006). Biosensor and bioelectrochemistry. **Current Opinion in Chemical Biology**, 10, 177-184

[14] Sassolas, A., Bouvier, B.D. and Blum, L.J. (2008). DNA Biosensors and microarrays. **Chemical Reviews,** 108, 109-139

[15] Nielsen, P. E., Egholm, M., Berg, R. H. and Buchardt, O. (1991). Sequence-selective recognition of DNA by strand displacement with a thymine-substituted polyamide. **Science,** 254, 1497–1500.

[16] Boontha, B., Nakkuntod, J., Hirankarn, N., Chaumpluk, P. and Vilaivan, T. (2008). Multiplex mass spectrometric genotyping of single nucleotide polymorphisms employing pyrrolidinyl peptide nucleic acid in combination with ion-exchange capture. **Analytical Chemistry**, 80, (21), 8178–8186.

[17] Cheng, M.M.C., Cuda, G., Bunimovich, Y.L., Gaspari, M., Heath, J.R., Hill, H.D., et al. (2006). Nanotechnologies for biomolecular detection and medical dignostics. **Current Opinion in Chemical Biology**, 10, 11-19

[18] Laconte, L., Nitin, N. and G., B. (2005). Magnetic nanoparticle probes. **Materials Today,** 8, (5), 32-38.

[19] Watson, J. D. and Crick, F.H.C. (1953). Genetical Implications of The Structure of Deoxyribonucleic Acid. **Nature**, 171, 964-967.

[20] Watson, J. D. and Crick, F.H.C. (1953). A Structure for Deoxyribose Nucleic Acid. **Nature**, 171, 737-738.

[21] Kool, E.T., Morales, J.C. and Guckian, K. (2000). Mimicking the Structure and Function of DNA: Insights into DNA Stability and Replication. **Angewandte Chemie International Edition**, 39, (6), 990-1009.

[22] Schweitzer, B. A. and Kool, E. T. (1995). Hydrophobic, Non-Hydrogen-Bonding Bases and Base Pairs in DNA. **Journal of the Americal Chemical Society**, 117, 737-738.

[23] Nielsen, P. E., Egholm, M., Berg, R. H. and Buchardt, O. (1991). Sequence-selective recognition of DNA by strand displacement with a thymine-substituted polyamide. **Science,** 254, 1497–1500.

[24] Egholm, M., Buchardt, O., Christensen, C., Freier, S. M., Driver, D. A., Berg, R. H., Kim, S. K., Norden, B. and Nielsen, P. E. (1993). PNA Hybridizes to Complementary Oligonucleotides Obeying the Waton-Crick Hydrogen Bonding Rules. **Nature,** 365, 566-568.

[25] Ray, A. and Norde, B. (2000). Peptide nucleic acid (PNA): its medical and biotechnical applications and promise for the future. **Federation of American Societies for Experimental Biology**, 14, 1041-1060

[26] Wang, J. (2005). Carbon-Nanotube Based Electrochemical Biosensors: A Review. **Electroanalysis,** 17, (1), 7-14.

[27] Gao, Z., Agarwal, A., Trigg, A. D., Singh, N., Fang, C., Tung, C. H., Fan, Y., Buddharaju, K. D. and Kong, J. (2007). Silicon Nanowire Arrays for Label-Free Detection of DNA. **Analytical Chemistry**, 79, 3291-3297

[28] Rosi, N. L. and Mirkin, C. A. (2001). Nanostructures in Biodiagnostica. **Chemical Reviews**, 105, 547-1562.

[29] Tansil, N. C. and Gao, Z. (2006). Nanoparticles in Biomolecular Detection. **Nanotoday**, 1, (1), 28-37.

[30] Shen, L., Stachowiak, A., Fateen, S. E. K., Laibinis, P. E. and Hatton, T. A. (2001). Structure of Alkanoic Acid Stabilized Magnetic Fluids. A Small-Angle Neutron and Light Scattering Analysis. **Langmuir**, 17, 288-299.

[31] Gupta, A. K. and Gupta, M. (2005). Synthesis and Surface Engineering of Iron Oxide Nanoparticles for Biomedical Applications. **Biomaterials,** 26, 3995–4021.

[32] Gamarra, L. F., Brito, G. E. S., Pontuschka, W. M., Amaro, E., Parma, A. H. C. and Goya, G. F. (2005). Biocompatible Superparamagnetic Iron Oxide Nanoparticles used for Contrast agents: A Structural and Magnetic Study. **Journal of Magnetism and Magnetic Materials**, 289, 439–441.

[33] Zhang, J. and Misra, R. D. K. (2007). Magnetic Drug-Targeting Carrier Encapsulated with Thermosensitive Smart Polymer: Core–Shell Nanoparticle Carrier and Drug Release Response. **Acta Biomaterialia**, 3, 838–850.

[34] Fortin, J. P., Wilhelm, C., Servais, J., Menager, C., Bacri, J. C. and Gazeau, F. (2007). Size-Sorted Anionic Iron Oxide Nanomagnets as Colloidal Mediators for Magnetic Hyperthermia. **Journal of the American Chemical Society**, 129, 2628-2635.

[35] Obata, K., Tajima, H., Yohda, M. and Matsunaga, T. (2002). Recent Developments in Laboratory Automation using Magnetic Particles for Genome Analysis. **Pharmacogenomics**, 3, (5), 697-708.

[36] Safarik, I. and Safarikova, M. (2004). Magnetic Techniques for the Isolation and Purification of Proteins and Peptides. **BioMagnetic Research and Technology**, 2, 7-24.

[37] Liberti, P. A., Rao, C. G. and Terstappen, L. W. M. M. (2001). Optimization of Ferrofluids and Protocols for the Enrichment of Breast Tumor Cells in Blood. **Journal of Magnetism and Magnetic Materials**, 225, 301-307.

[38] Gao, J., Gu, H. and Xu, B. (2009). Multifunctional Magnetic Nanoparticles: Design, Synthesis, and Biomedical Applications. **Accounts of Chemical Research**, 42, 1097-1107.

[39] Kikuchi, T., Kasuya, R., Endo, S., Nakamura, A., Takai, T., Nolte, N. M., Tohji, K. and Balachandran, J. (2011). Preparation of Magnetite Aqueous Dispersion for Magnetic Fuid Hyperthermia. **Journal of Magnetism and Magnetic Materials**, 323, 1216–1222.

[40] Carpenter, E. E., Sangregono, C. and O'Connor, C. J. (1999). Effects of Shell Thickness on Blocking Temperature of Nanocomposites of Metal Particles With Gold Shells. **IEEE Transactions on Magnetics**, 35, 3496-3498

[41] O'Connor, C. J., Kolesnichenkoa, V., Carpenter, E., Sangregorioc, C., Zhoua, W., Kumbhar, A., Sims, J. and Agnoli, F. (2001). Fabrication and Properties of Magnetic Particles with Nanometer Dimensions. **Synthetic Metals**, 122, 547–557.

[42] Stolnik, S., Illum, L. and Davis, S. S. (1995). Long Circulating Microparticulate Drug Carriers. **Advanced Drug Delivery Reviews**, 16, 195-214.

[43] Kim, D. K., Zhang, Y., Voit, W., Rao, K. V. and Muhammed, M. (2001). Synthesis and Characterization of Surfactant-Coated Superparamagnetic Monodispersed Iron Oxide Nanoparticles. **Journal of Magnetism and Magnetic Materials**, 225, 30-36.

[44] Lee, D. K., Kang, Y. S., Lee, C. S. and Stroeve, P. (2002). Structure and Characterization of Nanocomposite Langmuir Blodgett Films of Pol(maleicmonoester)/Fe3O4 Nanoparticle Complexes. **The Journal of Physical Chemistry B**, 106, 7267-7271.

[45] Veiseh, O., Gunn, J. W. and Zhang, M. (2010). Design and Fabrication of Magnetic Nanoparticles for Targeted Drug Delivery and Imaging. **Advanced Drug Delivery Reviews**, 62 284–304.

[46] Hayashi, K., Ono, K., Suzuki, H., Sawada, M., Moriya, M., Sakamoto, W. and Yogo, T. (2010). One-Pot Biofunctionalization of Magnetic Nanoparticles via Thiol-Ene Click Reaction for Magnetic Hyperthermia and Magnetic Resonance Imaging. **Chemistry of Materials**, 22, 3768–3772.

[47] Wang, T. H. and Lee, W. C. (2003). Immobilization of Proteins on Magnetic Nanoparticle. **Biotechnology and Bioprocess Engineering**, 8, (4), 263-267.

[48] Pan, B. F., Gao, F. and Gu, H. C. (2005). Dendrimer Modified Magnetite Nanoparticles for Protein Immobilization. **Journal of Colloid and Interface Science,** 284, 1–6.

[49] Johnson, A. K., Zawadzka, A. M., Deobald, L. A., Crawford, R. L. and Paszczynski, A. J. (2008). Novel Method for Immobilization of Enzymes to Magnetic Nanoparticles. **Journal of Nanoparticle Research,** 10, 1009–1025.

[50] Sassolas, A., Leca-Bouvier, B. D. and Blum, L. J. (2008). DNA Biosensors and Microarrys. **Chemical Reviews**, 108, 109-139

[51] Willhelmasson, L. M., Norden, B., Mukherjee, K., Dulay, M.T., and Zare, R.N. (2002). Genetic Screening using the Colour Change of a PNA-DNA Hybrid Binding Cyanine Dye. **Nucleic Acids Research,** 30, (2), 1-4.

[52] Komiyama, M., Ye, S., Liang, X., Yamamoto, Y., Tomita, T., Zhou, J. M. and Aburatani, H. (2003). PNA for One-Base Differentiating Protecting of DNA from Nuclease and Its use for SNPs Detection. **Journal of the Americal Chemical Society**, 125, 3758-3762

[53] Zhang, N. and Appella, D. H. (2007). Colorimetric Detection of Anthrax DNA with a Peptide Nucleic Acid Sandwich-Hybridization Assay. **Journal of the American Chemical Society**, 129, 8424-8425.

[54] Svanvik, N., Weatman, G., Wang, D. and Kubista, M. (2000). Light-Up Probe: Thiazole-Orange-Conjugated Peptide Nucleic Acid for Detection of Target Nucleic Acid in Homogeneous Solution. **Analytical Biochemistry**, 281, 26-35.

[55] Socher, E., Jarikote, D. V., Knoll, A., Ruglin, L., Burmeister, J. and Seitz, O. (2008). FIT Probe: Peptide Nucleic Acid Probe with a Fluorescent Base Surrogate Enable real-time DNA Quantification and Single Nucleotide Polymorphism Discovery. **Analytical Biochemistry**, 375, 318-330.

[56] Gaylord, B. S., Heeger, A. J. and Bazan, G. C. (2002). DNA Detection using Water-Soluble Conjugated Polymers and Peptide Nucleic Acid Probe. **Proceedings of the National Academy of Sciences USA**, 99, 10954-10957.

[57] Zhang, G. J., Chua, J. H., Chee, R. E., Agarwal, A., Wong, S. M., Buddharaju, K. D. and Balasubramanian, N. (2008). Highly Sensitive Measurements of PNA-DNA Hybridization using Oxide-Etched Silicon Nanowire Biosensors. **Biosensors and Bioelectronics**, 23, 1701-1707

[58] Zhu, N., Zhang, A., He, P. and Fang, Y. (2004). DNA Hybridization at Magnetic Nanoparticles with Electrochemical Stripping Detection. **Electroanalysis,** 16, (23), 1925-1930.

[59] Stoeva, S. I., Huo, F., Lee, J. S. and Mirkin, C. A. (2005). Three-Layer Composite Magnetic Nanoparticle Probes for DNA. **Journal of the American Chemical Society**, 127, 15362-15363.

[60] Dias, N. and Stein, C. A. (2002). Antisense Oligonucleotides: Basic Concepts and Mechanisms. **Molecular Cancer Therapeutics**, 1, 347–355.

[61] Kerman, K., Matsubara, Y., Morita, Y., Takamura, Y. and Tamiya, E. (2004). Peptide Nucleic Acid Modified Magnetic Beads for Intercalator Based Electrochemical Detection of DNA Hybridization. **Science and Technology of Advanced Materials**, 5, 351-367.

[62] Baucom, P. J. and Girard, J. E. (1997). DNA Typing of Human Leukocyte Antigen Sequence Polymorphisms by Peptide Nucleic Acid Probes and MALDI-TOF Mass Spectrometry. **Analytical Chemistry**, 69, 4894-4898.

[63] Wang, F., Shen, H., Feng, J. and Yang, H. (2006). PNA-Modified Magnetic Nanoparticles and Their Hybridization with Single-Stranded DNA Target: Surface Enhanced Raman Scatterings Study. **Microchim Acta**, 153, 15–20.

[64] Pita, M., J.M., A., Dominguez, C. V., Briones, C., Martí, M. E., Gago, J. A. M., Morales, M. P. and Fernández, V. M. (2008). Synthesis of cobalt ferrite core/metallic shell nanoparticles for the development of a specific PNA/DNA biosensor. **Journal of Colloid and Interface Science,** 32, 484–492.

[65] Prencipe, G., Maiorana, S., Verderio, P., Colombo, M., Fermo, P., Caneva, E., Prosperi, D. and Licandro, E.M. (2009). Magnetic Peptide Nucleic Acids for DNA Targeting. **Chemical Communications**, 6017–6019.

[66] Taylor, L. D., Kolesinski, H. D., Mehta, A. C., Locatell, L. and Larson, P. S. (1982). Synthesis of Poly(4,4-dimethyl-2-vinyl-5-oxazolone) an Interesting Material for Preparing Polymeric Agents. **Die Makromolekulare Chemie, Rapid Communications**, 3, 779 - 782.

[67] Rasmussen, J. K., Heilmann, S. M., Palensky, F. J., Smith, H. K., Melancon, K. C. and "Chemistry of alkenylactones" Makromol. Chem. Rapid Commun. 1984, 67-70. (1984). Chemistry of alkenylactones. **Die Makromolekulare Chemie, Rapid Communications**, 5, 67-70.

[68] Jennifer, A., Tripp, J. A., Stein, F. S. and M.J.F, J. (2000). "Reactive Filtration": Use of Functionalized Porous Polymer Monoliths as Scavengers in Solution-Phase Synthesis. **Organic Letters**, 2, (2), 195-198.

[69] Cho, M. J., Choi, D. H., Sullivan, P. A., Akelaitis, A. J. P. and Dalton, L. R. (2008). Recent Progress in Second-Order Nonlinear Optical Polymers and Dendrimers. **Progress in Polymer Science**, 33, (11), 1013-1058.

[70] Heilmann, S. M., Drtina, G. J., Haddad, L. C., Rasmussen, J. K., Gaddama, B. N., Liu, J. J., Fitzsimons, R. T., Fansler, D. D., Vyvyan, J. R., Yang, Y. N. and Beauchamp, T. J. (2004). Azlactone-Reactive Polymer Supports for Immobilizing Synthetically useful Enzymes Part I. Pig Liver Esterase on Dispersion Polymer Supports. **Journal of Molecular Catalysis B: Enzymatic**, 30, 33–42.

[71] Guyomard, A., Fournier, D., Pascual, S., Fontaine, L. and Bardeau, J. F. (2004). Prepation and Characterization of Azlactone Functionalized Polymer Supports and their Application as Scavengers. **European Polymer Journal**, 40, 2343-2348.

[72] Fournier, D., Pascual, S., Montembault, M., Haddleton, D. M. and Fontaine, L. (2006). Well-Defined Azlactone-Functionalized (Co)polymers on a Solid Support: Synthesis via Supported Living Radical Polymerization and Application as Nucleophile Scavengers. **Journal of Combinatorial Chemistry**, 8, 522-530.

[73] Cullen, S. P., Mandel, I. C. and Gopalan, P. (2008). Surface-Anchored Poly(2-vinyl-4,4-dimethyl azlactone) Brushes as Templates for Enzyme Immobilization. **Langmuir**, 24, 13701-13709.

[74] Fontaine, L., Lemele, T., Brosse, J. C., Sennyey, G., Senet, J. P. and Wattez, D. (2002). Grafting of 2-Vinyl-4,4-dimethylazlactone onto Electron-Beam Activated Poly(propylene) Films and Fabrics. Application to the Immobilization of Sericin. **Macromolecular Chemistry and Physics,** 203, 1377-1384.

[75] Barringer, J. E., Messman, J. M., Banaszek, A. L., Meyer, H. M. and Kilbey, S. M. (2009). Immobilization of Biomolecules on Poly(vinyldimethylazlactone)-Containing Surface Scaffolds. **Langmuir**, 25, 262-268.

[76] Prai-in, Y., Tankanya, K., Rutnakornpituk, B., Wichai, U., Montembault, V., Pascual, S., Fontaine, L., and Rutnakornpituk, M. (2012). Azlactone functionalization of magnetic nanoparticles using ATRP and their bioconjugation. **Polymer**, 52(1), 113-120

[77] Thomson, S.A., Josey, J.A., Cadilla, R., Gaul, M.D., Hassman, F., Luzzio, M.J., Pipe, A.J., Reed, K.L., Ricca, D.J., Wiethe, R.W. and Noble, S.A. (1995). Fmoc mediated synthesis of peptide nucleic acid. **Tetrahedron**, 51(22), 6179-6194.

[78] Dueholm, K.L., Egholm, M., Behrens, C., Christensen, L., Hansen, H.F., Vulpius, T., Petersen, K.H,Berg, R.H., Nielsen, P.E. and Buchardt, O. (1994). Synthesis of Peptide Nucleic Acid Monomers Containing the Four Natural Nucleobases: Thymine, Cytosine, Adenine, and Guanine and Their Oligomerization. **The Journal of Organic Chemistry**, 59, 5767-5773.

[79] Mukthung, C. (2007). **Synthesis and Investigation of Peptide Nucleic Acid Containing Carbazole Derivatives as Universal Base**. Phitsanulok: Naresuan University,

[80] Benchawan, T., Tantirungrotechai, Y., Woski, S.A. and Wichai, U. (2009). Computational design and synthesis of carbazole drivatives for investigation of universal base properties. In 35th Congress on Science and Technology of Thailand.

[81] Awasthi, S.K. and Nielsen, P.E. (2002). Parallel synthesis of PNA-peptide conjugate libraries. **Combinatorial Chemistry and High Throughput Screening,** 5, 253-249

[82] Kim, B. and Sigmund, W.M. (2004) Functionalized multiwall carbon nanotube/gold nanoparticle composites. **Langmuir,** 20, 8239-8242

[83] Cai, X., Zhang, Y. and Wu, G. (2011). A novel approach to prepare PA6/Fe_3O_4 Microspheres for Protein immobilization. **Journal of Applied Polymer Science,** 122, 2271-2277

[84] Lim, S.H., Bestvater, F., Buchy, P., Mardy, S. and Yu, A.D.C. (2009). Quantitative analysis of nucleic acid hybridization on magnetic particles and quantum dot-based probes. **Sensors**, 9, 5590-5599.

[85] Zhong, X., Reynolds, R., Kidd, J.R., Kidd,.K.K., Jenison, R., Marlar, R.A. and Ward, D.C. (2003). Single-nucleotide polymorphism genotyping on optical thin-film biosensor chips. **Proceedings of the National Academy of Sciences USA,** 100 (20), 11559–11564.

[86] Su, X. and Kanjanawarut, R. (2009). Control of metal nanoparticles aggregation and dispersion by PNA and PNA-DNA complexes, and its application for colorimetric DNA detection. **American Chemical Society Nano,** 3 (9), 2751–2759.

[87] Nielsen, P.E. (2004). **Peptide nucleic acids: protocols and applications** (2^{nd}). U.K.: Horizon Bioscience.

[88] Singh, J.S. (2008). FTIR and Raman spectra and fundamental frequencies of biomolecule: 5-Methyluracil (thymine). **Journal of Molecular Structure,** 876, 127–133

[89] Xavier, C., Pak, J.K., Santons, I. and Alcerto, R. (2007) Evaluation of two chelator a PNA monomer with the *fac*-$[^{99m}Tc(CO)_3]^+$ moiety. **Journal of Organometallic Chenistry**, 692, 1332-1339

APPENDIX

APPENDIX A: ^{1}H and ^{13}C NMR Spectra, MALDI-TOF mass spectra HPLC Chromatogram

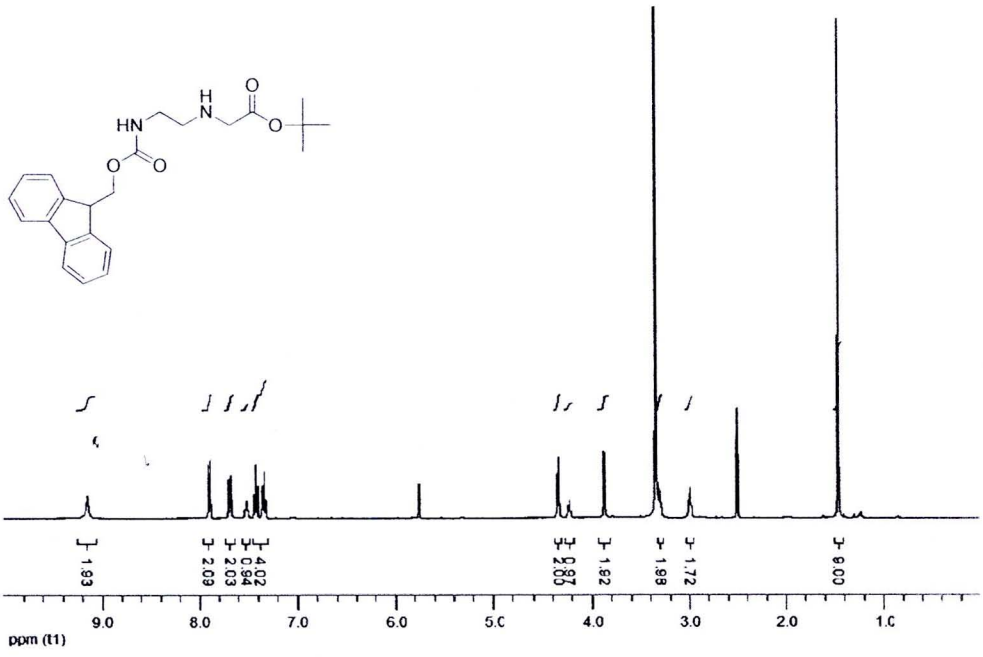

Figure 48 ^{1}H NMR spectrum of *tert*-Butyl *N*-[2-(*N'*-9-fluorenylmethoxycarbonyl) aminoethyl]glyeinate hydrochioride (40) (DMSO-d_6)

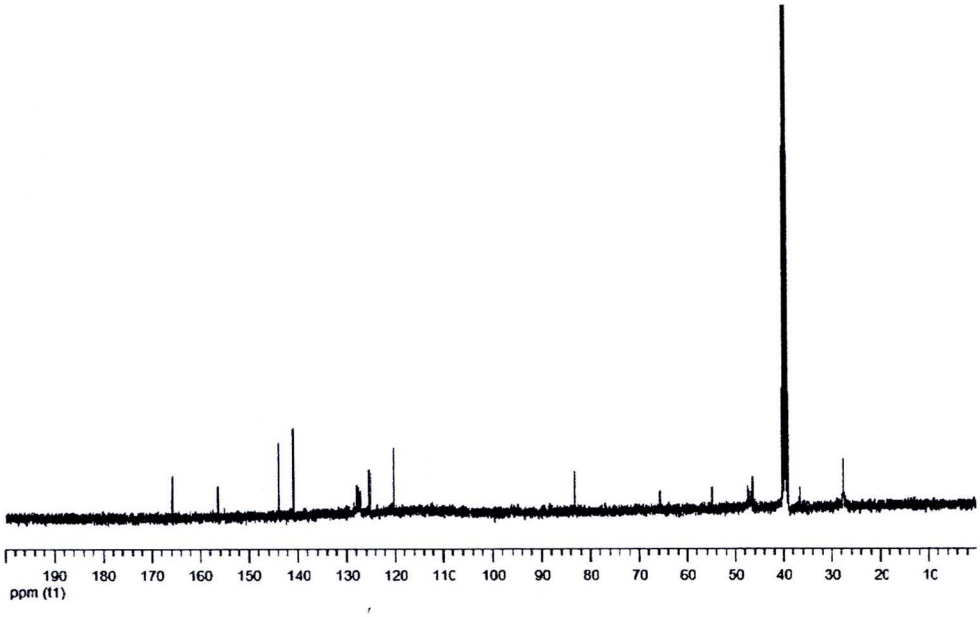

Figure 49 ^{13}C NMR spectrum of *tert*-Butyl *N*-[2-(*N'*-9-fluorenylmethoxycarbonyl) aminoethyl] glyeinate hydrochioride (40) (DMSO-d_6)

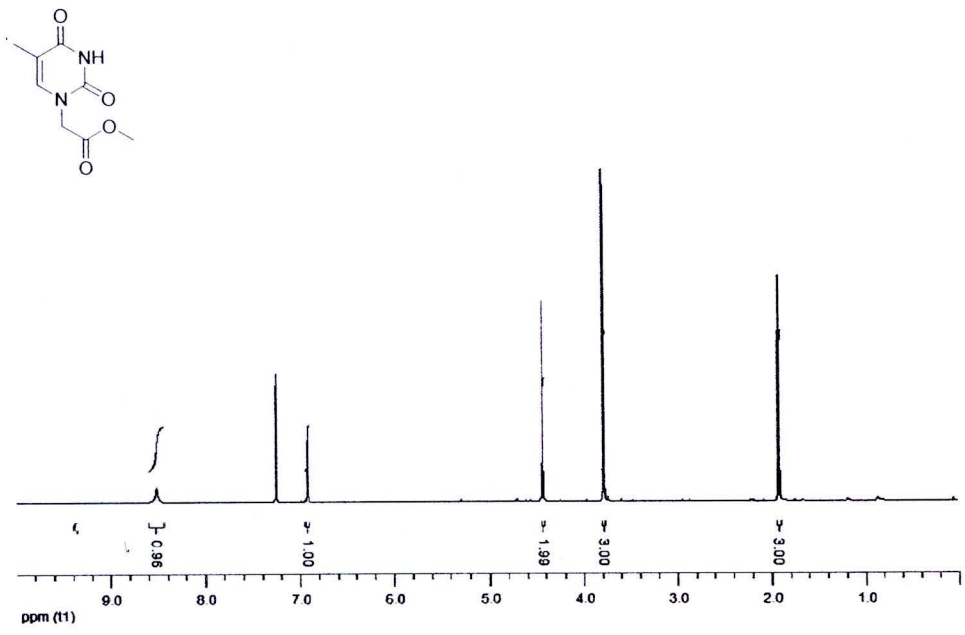

Figure 50 ^{1}H NMR spectrum of thymine-1-yl-methyl acetate (43) ($CDCl_3$)

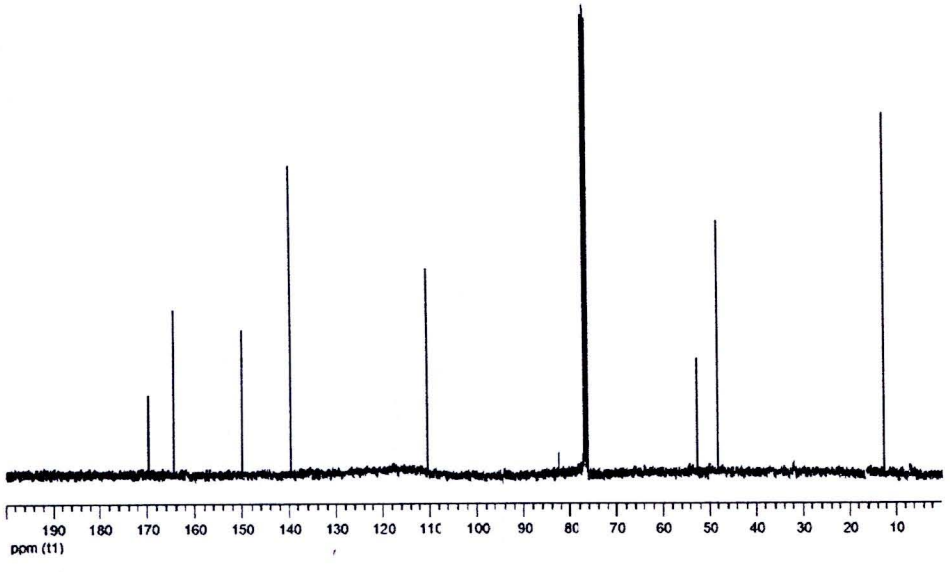

Figure 51 ^{13}C NMR spectrum of thymine-1-yl-methyl acetate (43) ($CDCl_3$)

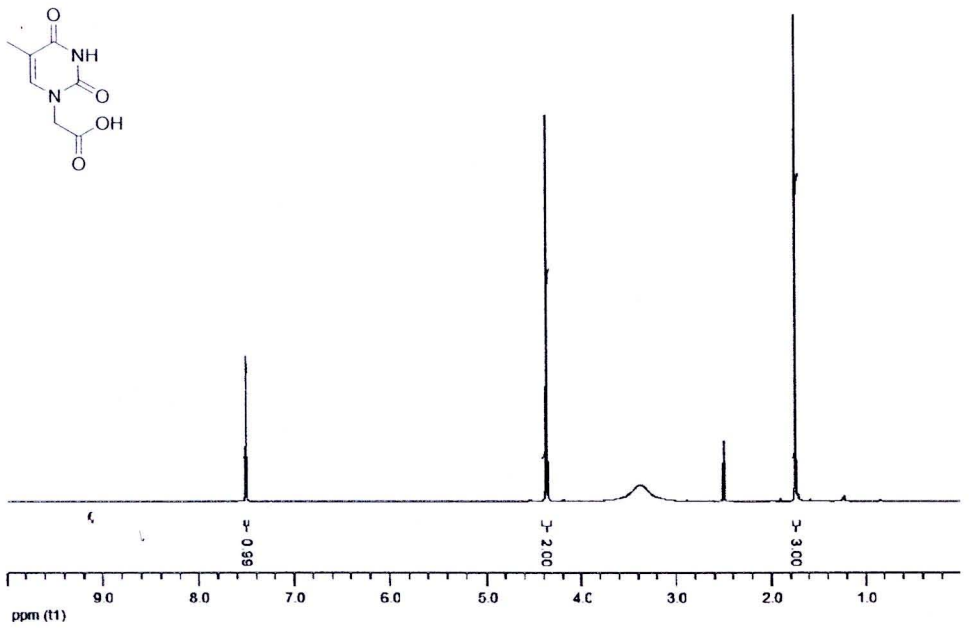

Figure 52 ^{1}H NMR spectrum of thymine-1-yl-acetic acid (44) (DMSO-d_6)

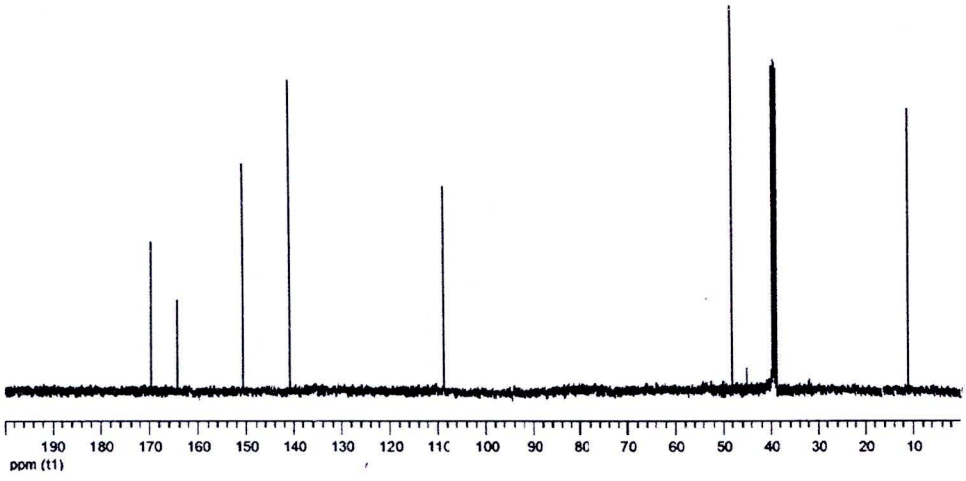

Figure 53 ^{13}C NMR spectrum of thymine-1-yl-acetic acid (44) (DMSO-d_6)

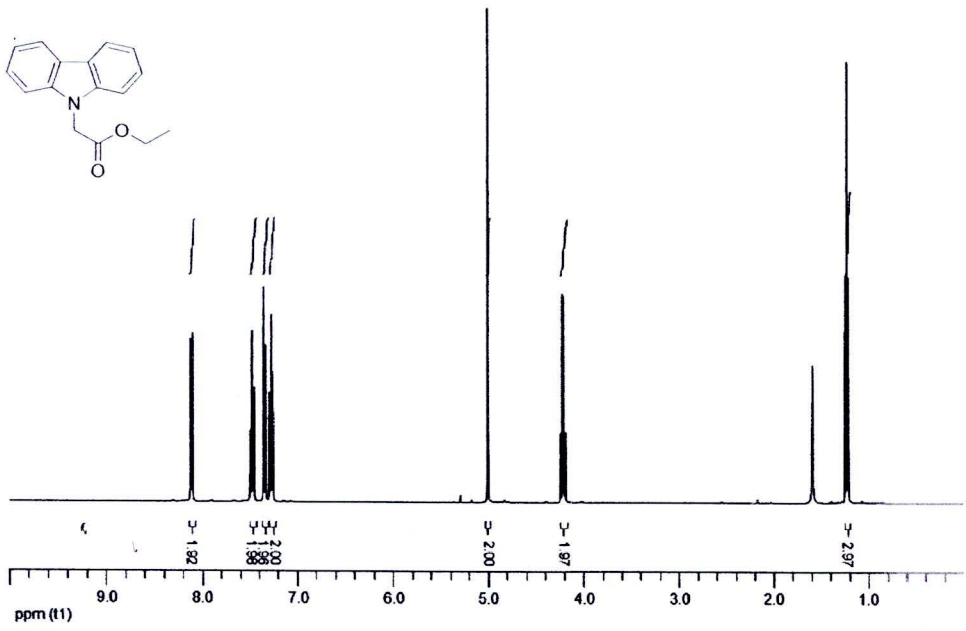

Figure 54 ^{1}H NMR spectrum of carbazole-9-yl-ethyl acetate (48) ($CDCl_3$)

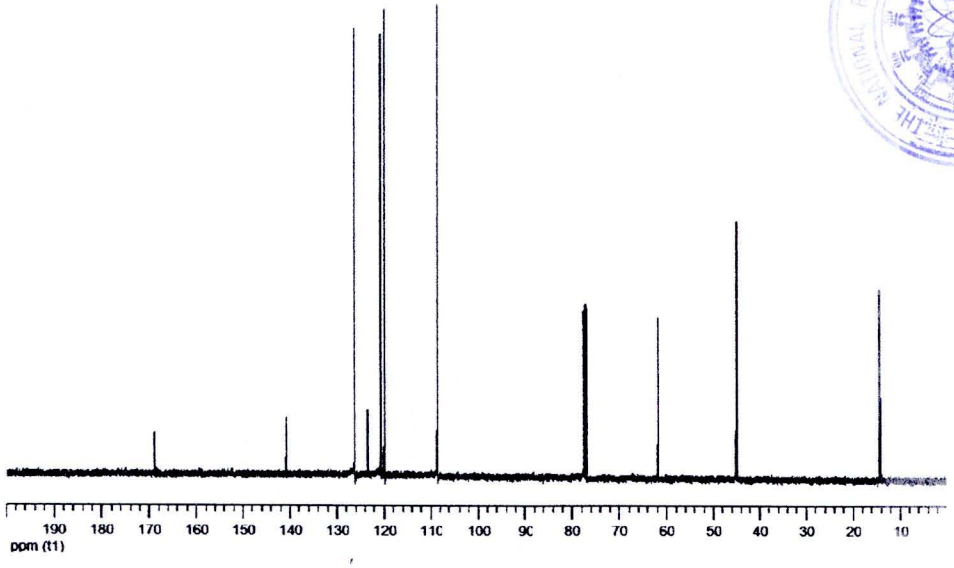

Figure 55 ^{13}C NMR spectrum of carbazole-9-yl-ethyl acetate (48) ($CDCl_3$)

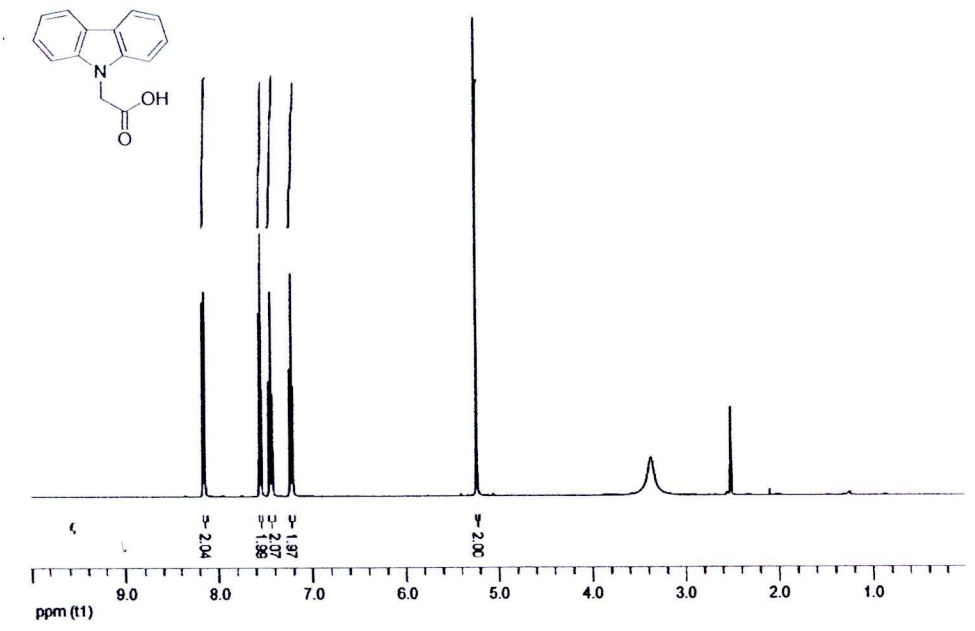

Figure 56 ^{1}H NMR spectrum of sarbazole-9-yl-acetic acid (47) (DMSO-d_6)

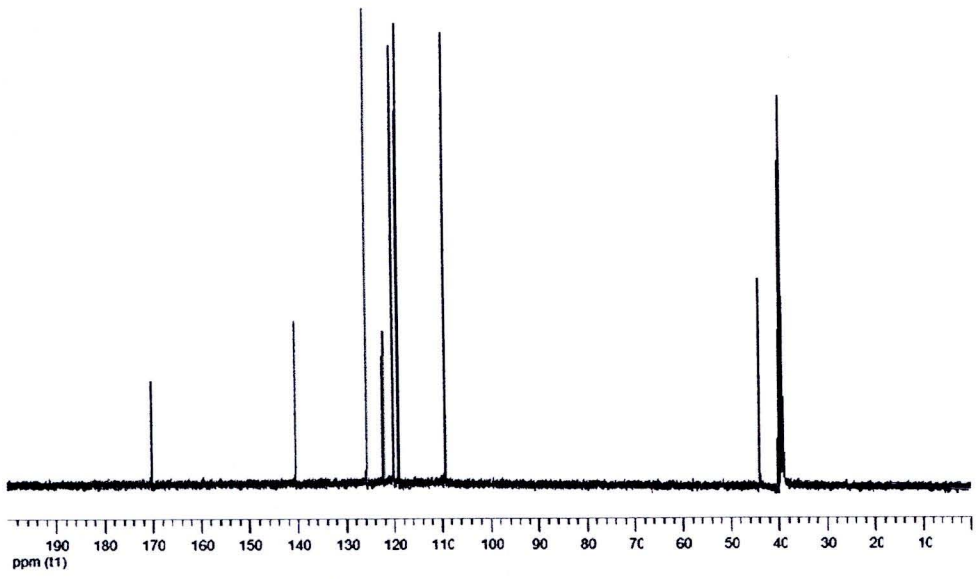

Figure 57 ^{13}C NMR spectrum of carbazole-9-yl-acetic acid (47) (DMSO-d_6)

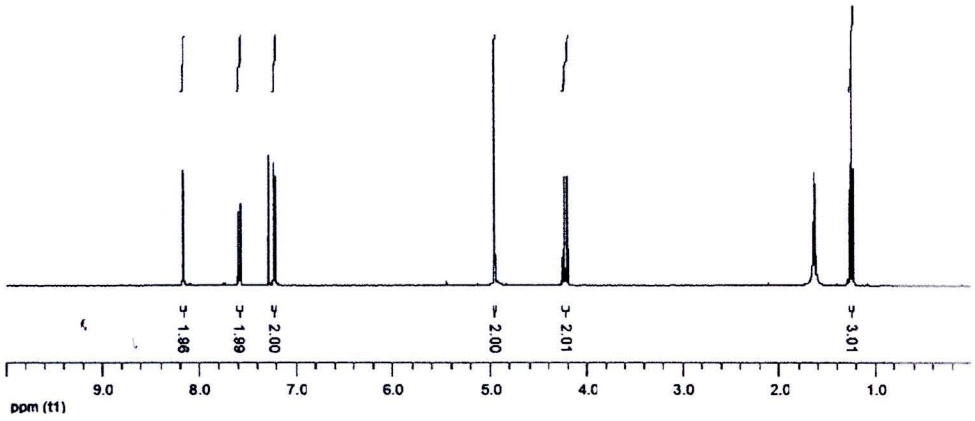

Figure 58 ^{1}H NMR spectrum of 3,6-dibromocarbazole-9-yl-ethyl acetate (49) ($CDCl_3$)

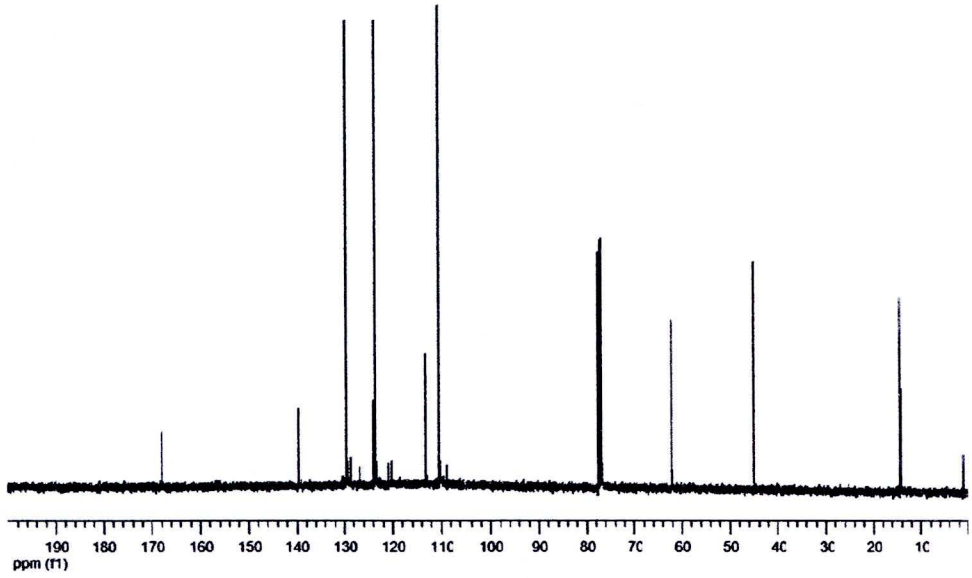

Figure 59 ^{13}C NMR Spectrum of 3,6-dibromocarbazole-9-yl-ethyl acetate (49) ($CDCl_3$)

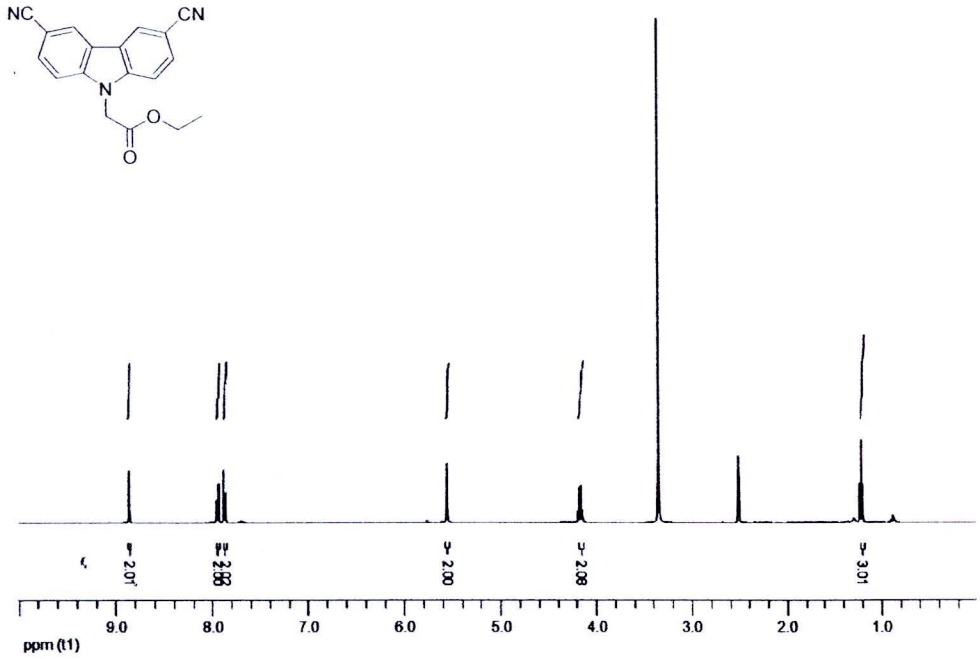

Figure 60 ^{1}H NMR spectrum of 3,6-dicyanocarbazole-9-yl-ethyl acetate (50) (DMSO-d_6)

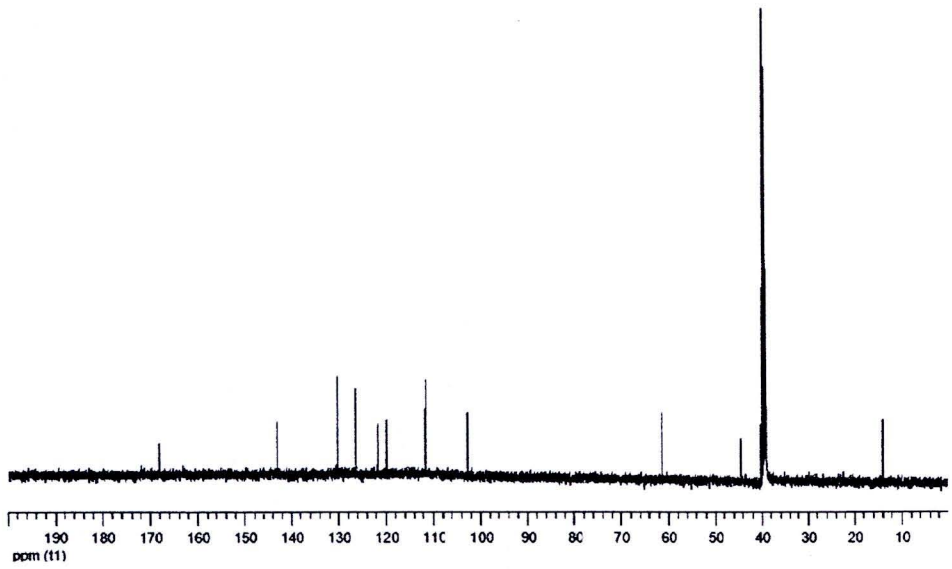

Figure 61 ^{13}C NMR spectrum of 3,6-dicyanocarbazole-9-yl-ethyl acetate (50) (DMSO-d_6)

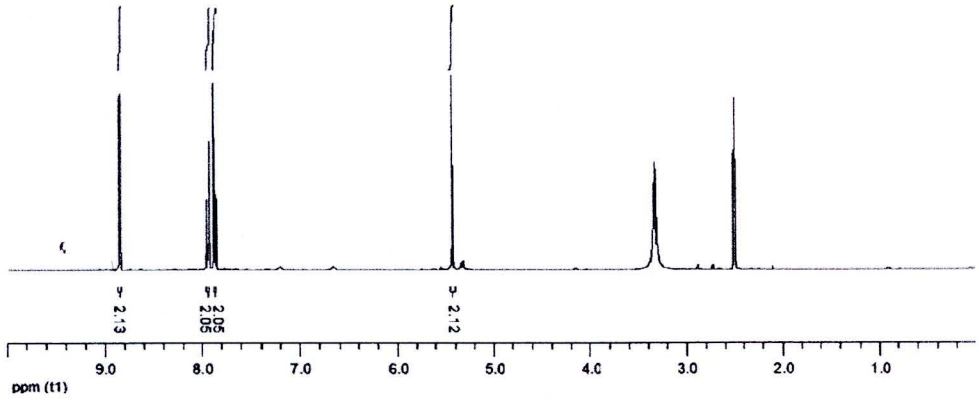

Figure 62 ^{1}H NMR spectrum of 3,6-dicyanocarbazole-9-yl-acetic acid (51) (DMSO-d_6)

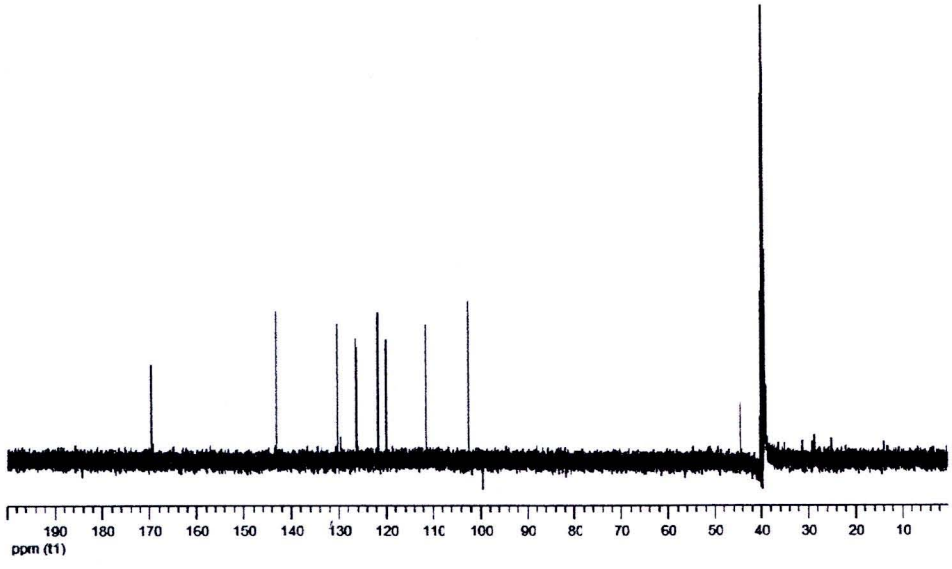

Figure 63 ^{13}C NMR spectrum of 3,6-dicyanocarbazole-9-yl-acetic acid (51) (DMSO-d_6)

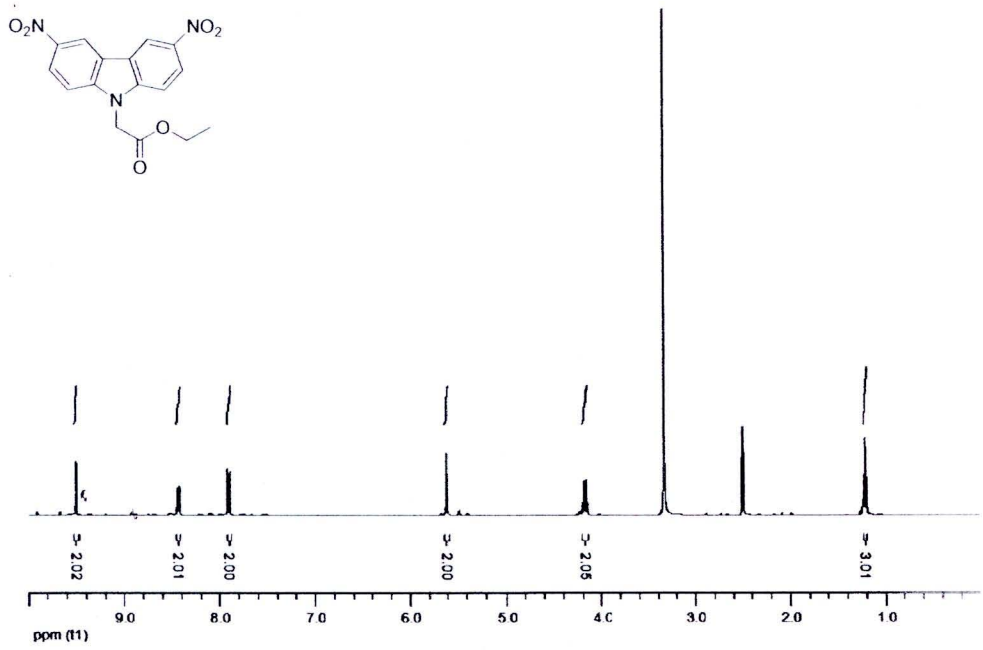

Figure 64 ^{1}H NMR spectrum of 3,6-dinitrocarbazole-9-yl-ethyl acetate (52) (DMSO-d_6)

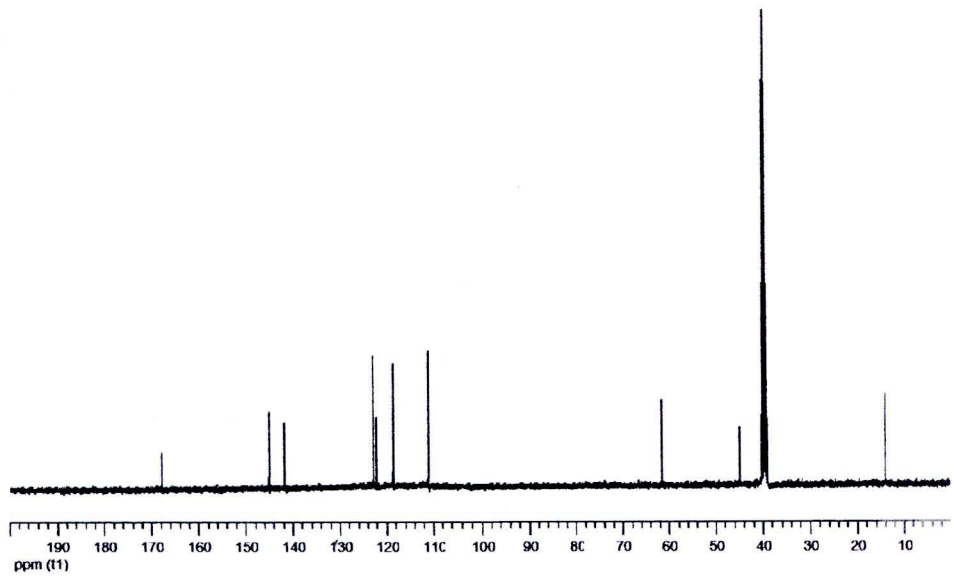

Figure 65 ^{13}C NMR spectrum of 3,6-dinitrocarbazole-9-yl-ethyl acetate (52) (DMSO-d_6)

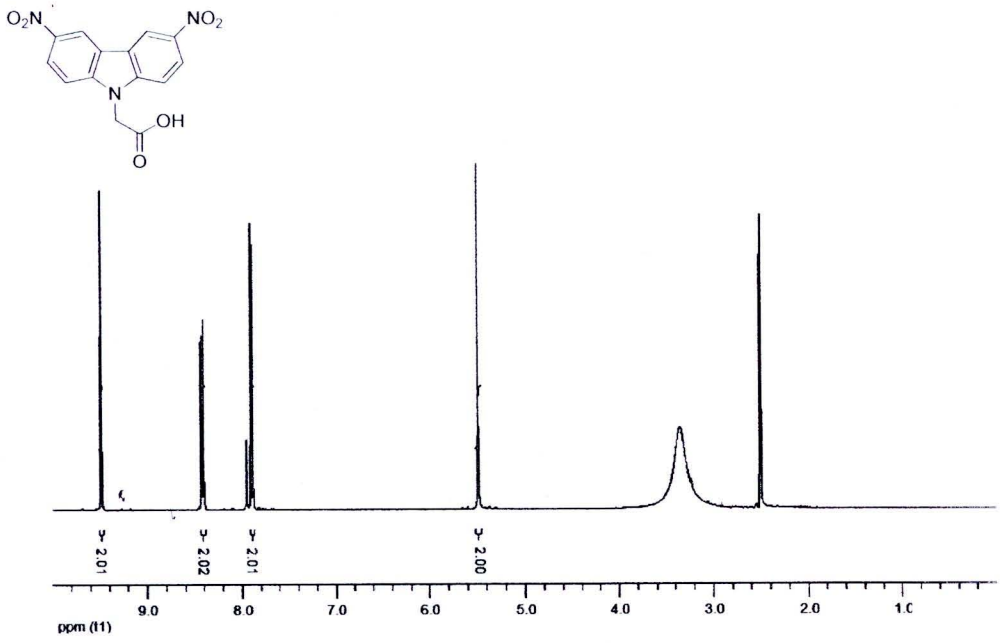

Figure 66 ^{1}H NMR spectrum of 3,6-dinitrocarbazole-9-yl-acetic acid (53) (DMSO-d_6)

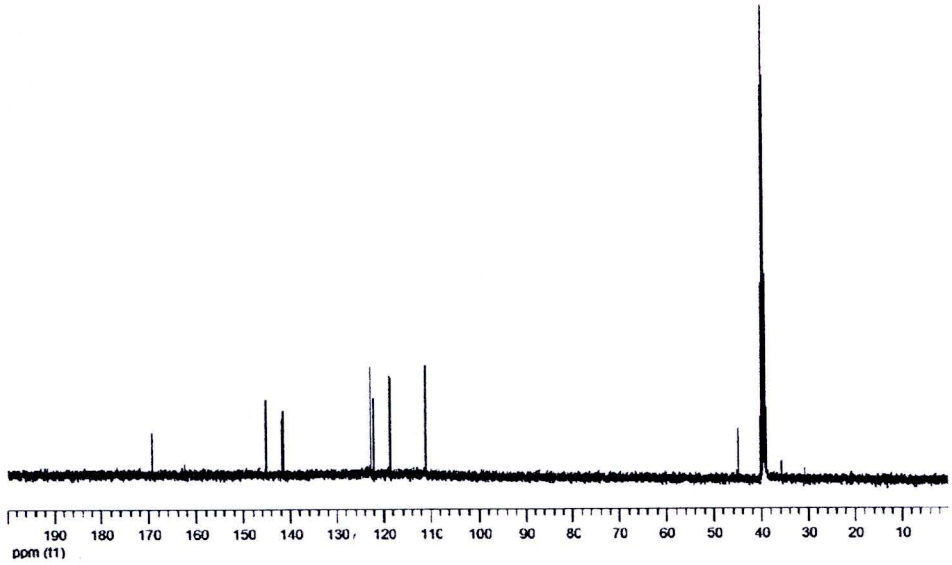

Figure 67 ^{13}C NMR spectrum of 3,6-dinitrocarbazole-9-yl-acetic acid (53) (DMSO-d_6)

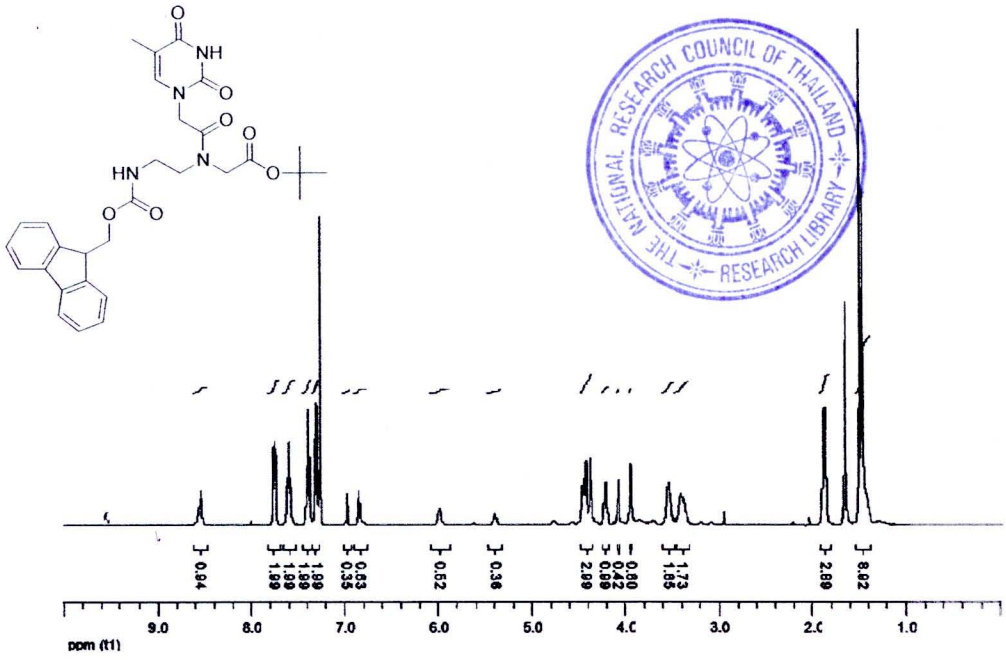

Figure 68 ^{1}**H NMR spectrum of *tert*-Butyl *N*-[2-(*N'*-9 fluorenylmethoxycarbonyl) aminoethyl]-*N*-[(thymine-1-yl)acetyl]glycinate (54a) ($CDCl_3$)**

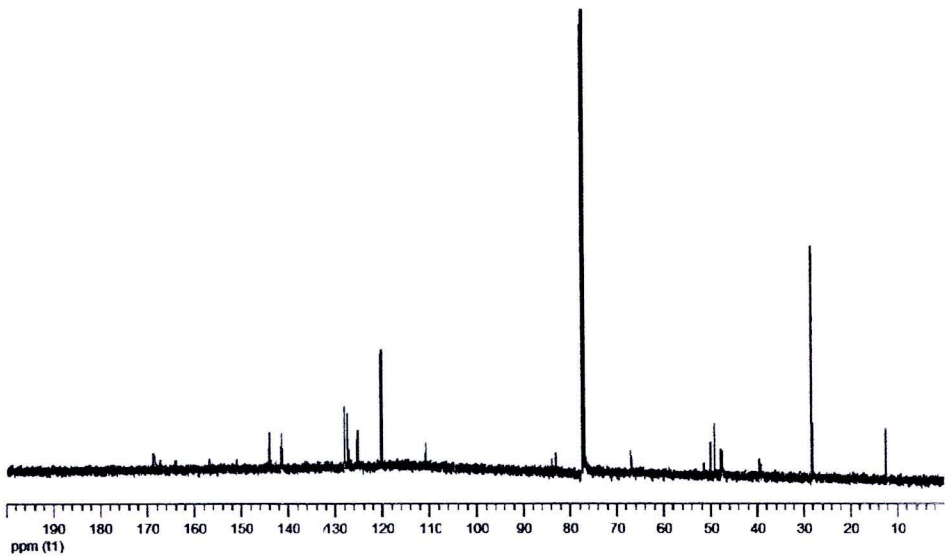

Figure 69 ^{13}**C NMR spectrum of *tert*-Butyl *N*-[2-(*N'*-9 fluorenylmethoxycarbonyl) aminoethyl]-*N*-[(thymine-1-yl)acetyl]glycinate (54a) ($CDCl_3$)**

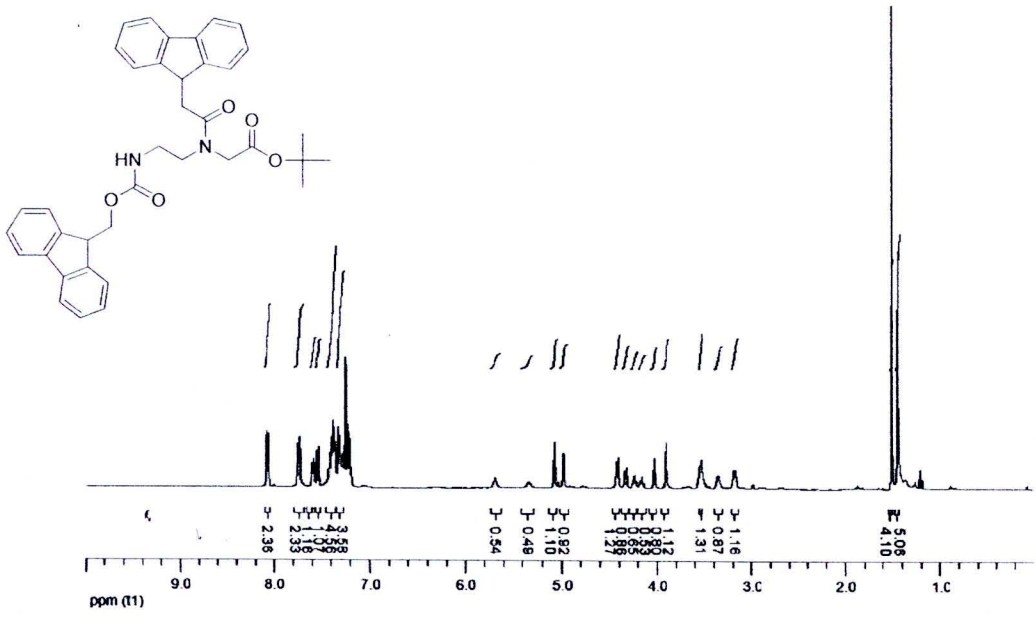

Figure 70 ^{1}H NMR spectrum of *tert*-Butyl *N*-[2-(*N'*-9 fluorenylmethoxycarbonyl) aminoethyl]-*N*- [(carbazole-9-yl)acetyl]glycinate (54b) ($CDCl_3$)

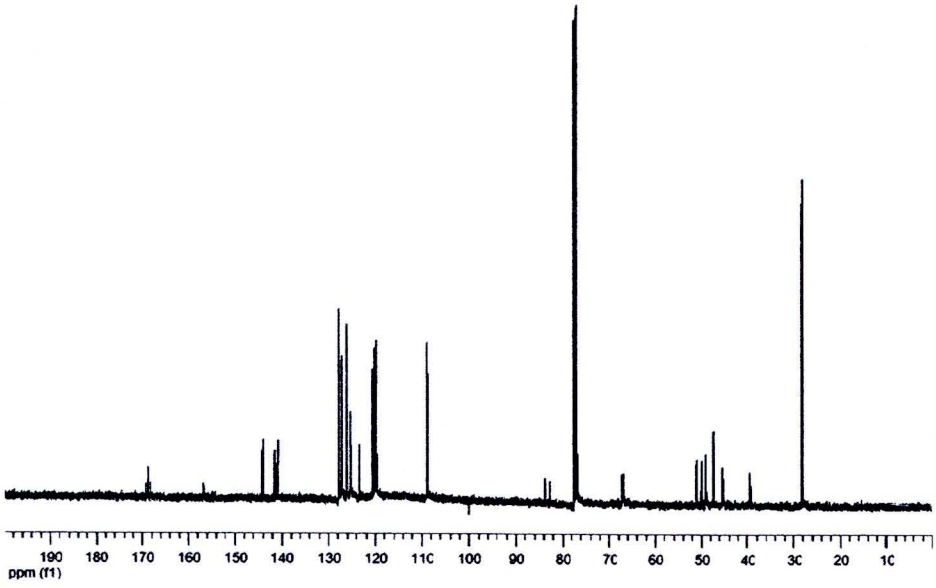

Figure 71 ^{13}C NMR spectrum of *tert*-Butyl *N*-[2-(*N'*-9 fluorenylmethoxycarbonyl) aminoethyl]-*N*- [(carbazole-9-yl)acetyl]glycinate (54b) ($CDCl_3$)

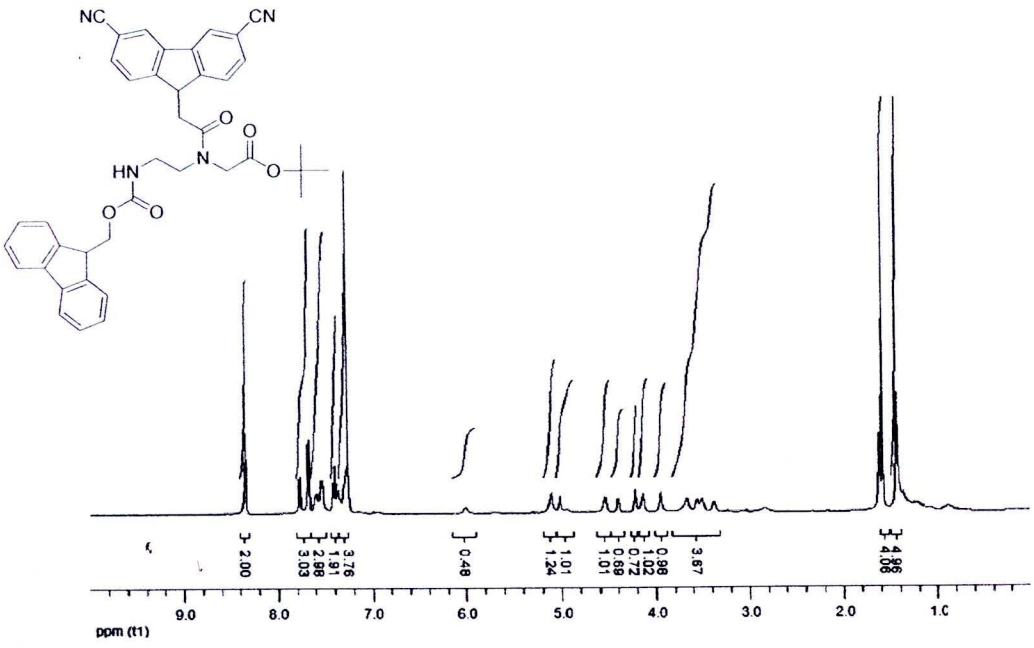

Figure 72 ^{1}H NMR spectrum of *tert*-Butyl *N*-[2-(*N'*-9 fluorenylmethoxycarbonyl) aminoethyl]-*N*- [(3,6-dicyanocarbazole-9-yl)acetyl]glycinate (54c) ($CDCl_3$)

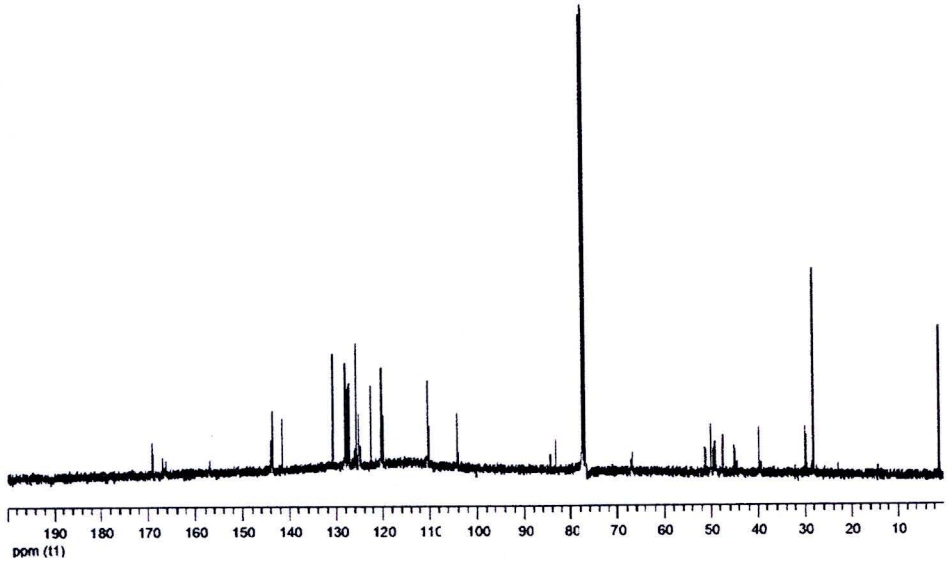

Figure 73 ^{13}C NMR spectrum of *tert*-Butyl *N*-[2-(*N'*-9 fluorenylmethoxycarbonyl) aminoethyl]-*N*- [(3,6-dicyanocarbazole-9-yl)acetyl]glycinate (54c) ($CDCl_3$)

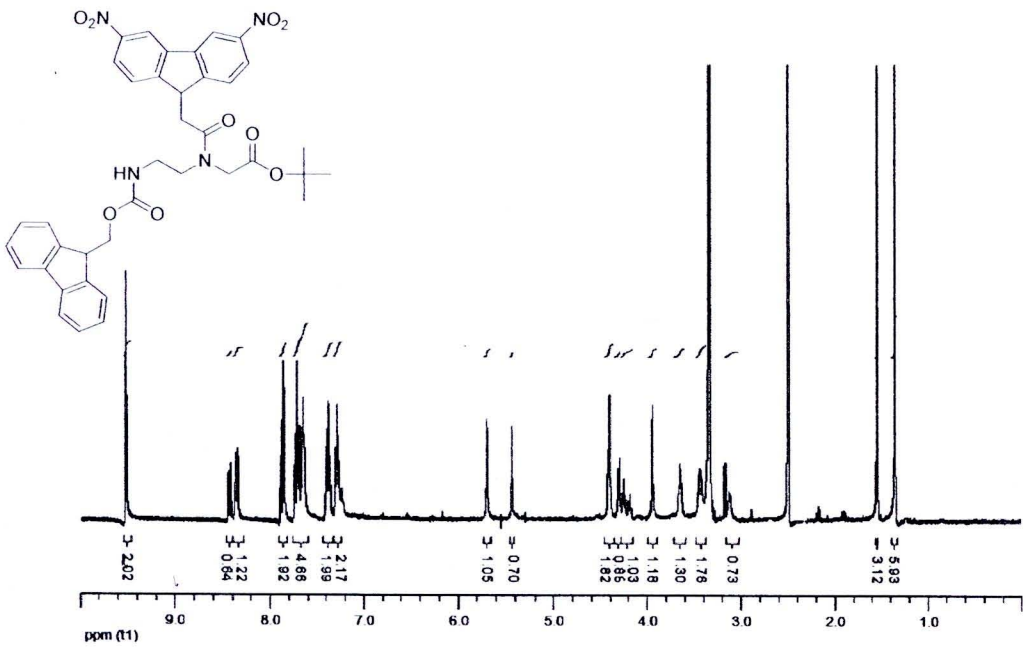

Figure 74 ^{1}H NMR spectrum of *tert*-Butyl *N*-[2-(*N'*-9 fluorenylmethoxycarbonyl) aminoethyl]-*N*-[(3,6-dinitrocarbazole-9-yl)acetyl]glycinate (54d) (DMSO-d_6)

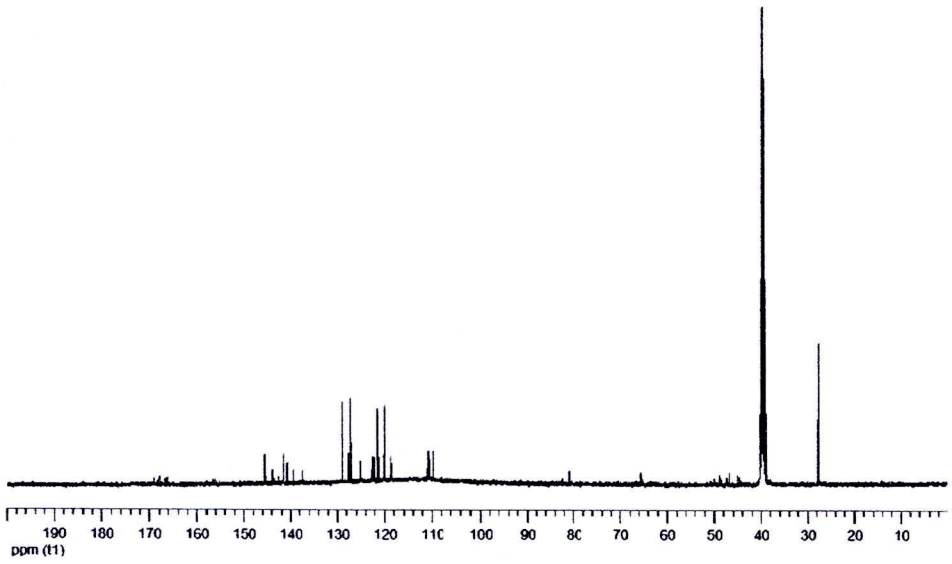

Figure 75 ^{13}C NMR spectrum of *tert*-Butyl *N*-[2-(*N'*-9 fluorenylmethoxycarbonyl) aminoethyl]-*N*-[(3,6-dinitrocarbazole-9-yl)acetyl]glycinate (54d) (DMSO-d_6)

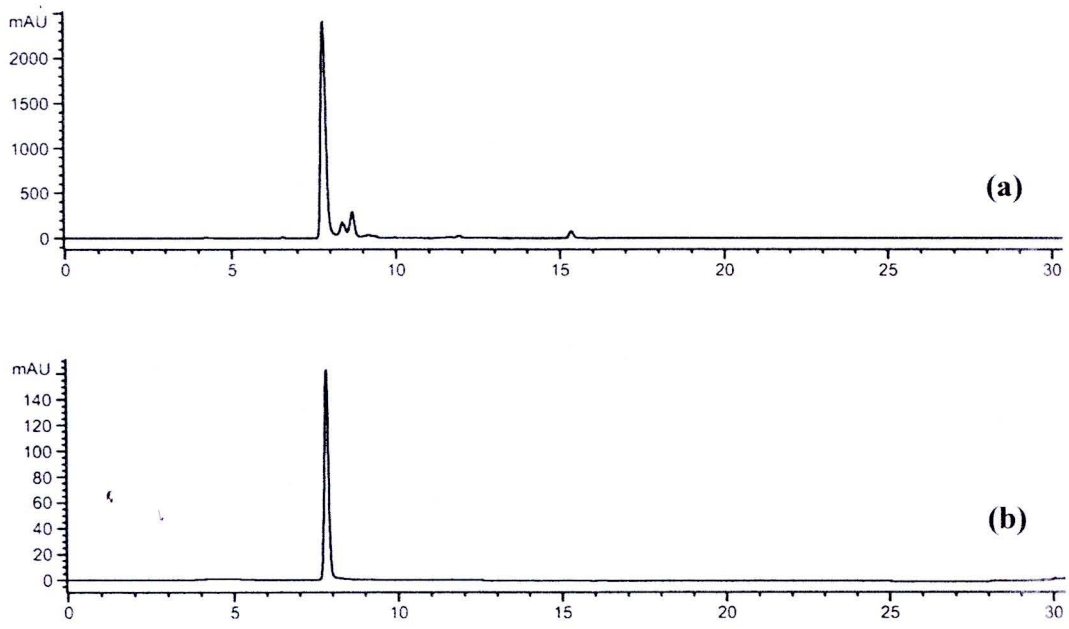

Figure 76 HPLC chromatogram of (a) crude and (b) purified NH_2-TT-$COONH_2$ (56a)

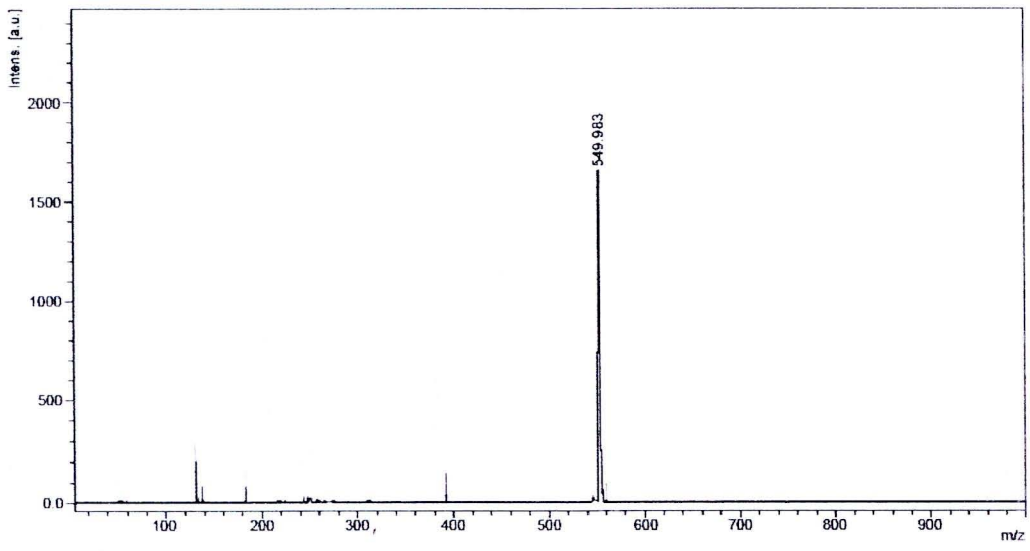

Figure 77 MALDI-TOF mass spectrum of purified NH_2-TT-$COONH_2$ (56a)

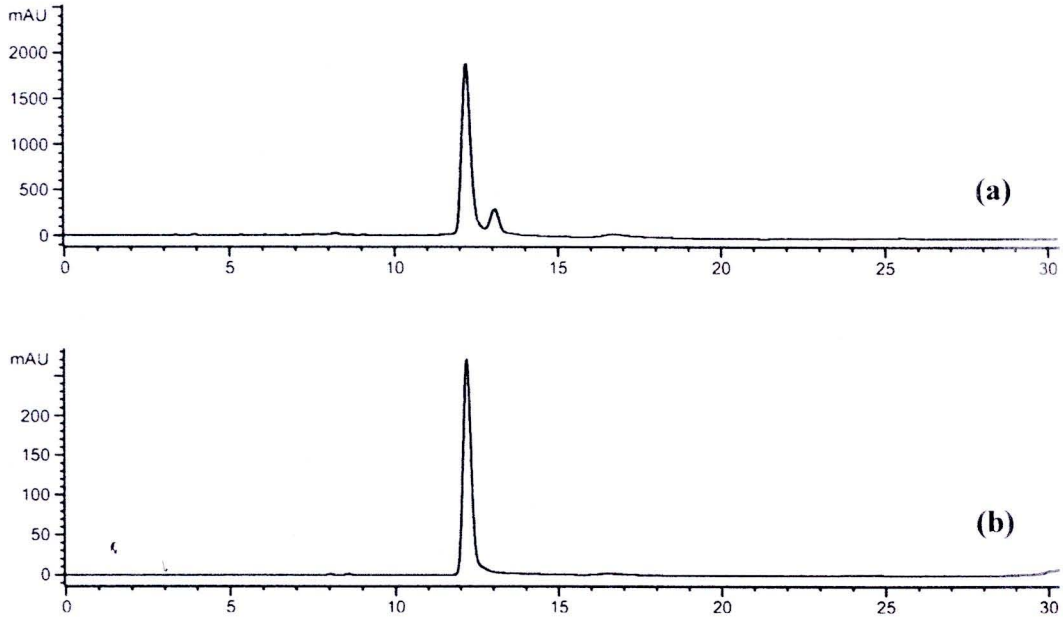

Figure 78 HPLC chromatogram of (a) crude and (b) purified NH_2-TTTT-$COONH_2$ (56b)

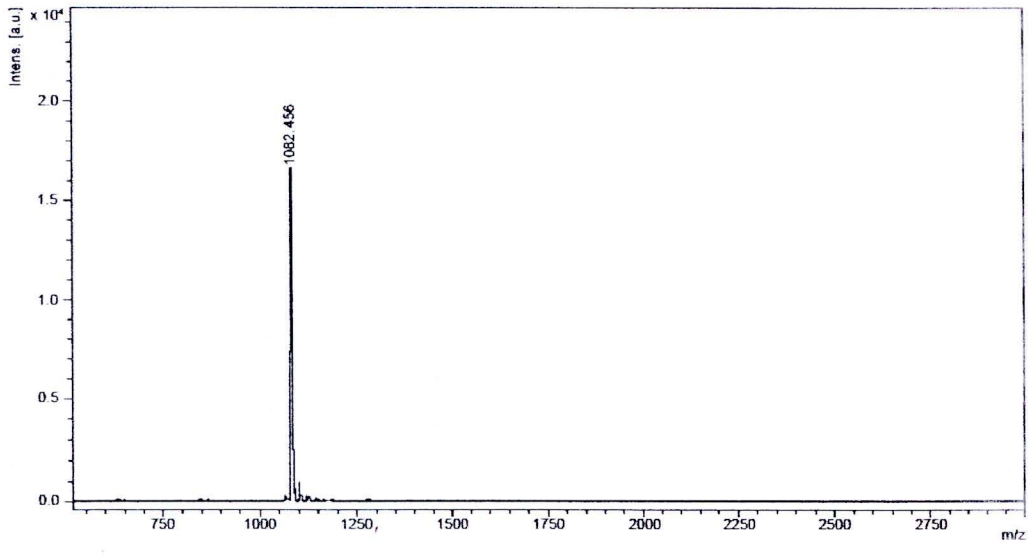

Figure 79 MALDI-TOF mass spectrum of purified NH_2-TTTT-$COONH_2$ (56b)

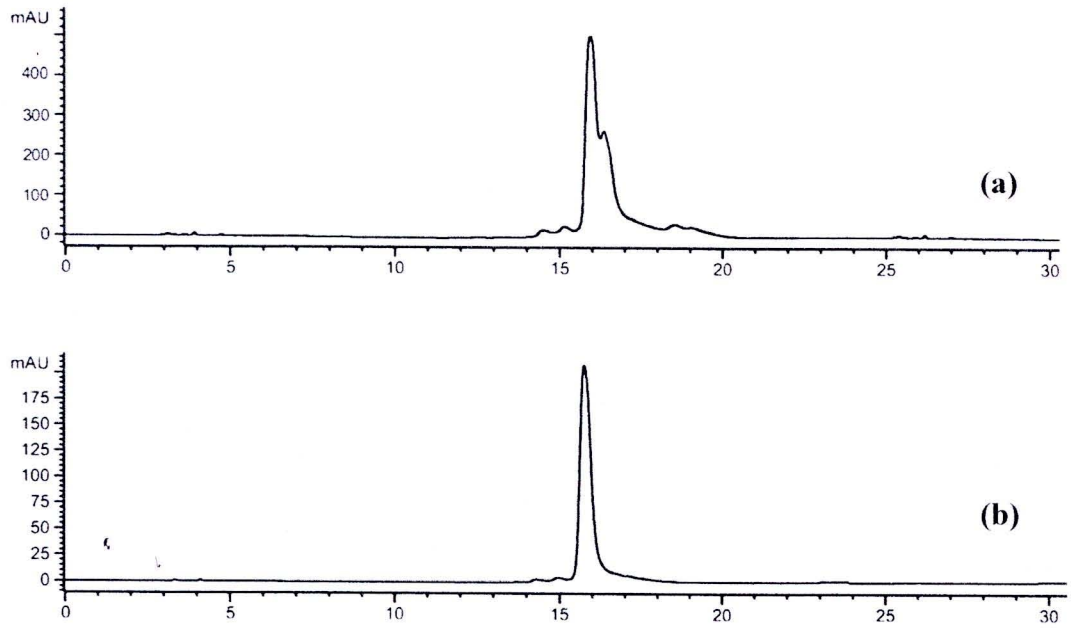

Figure 80 HPLC chromatogram of (a) crude and (b) purified NH_2-TTTTTT-$COONH_2$ (56c)

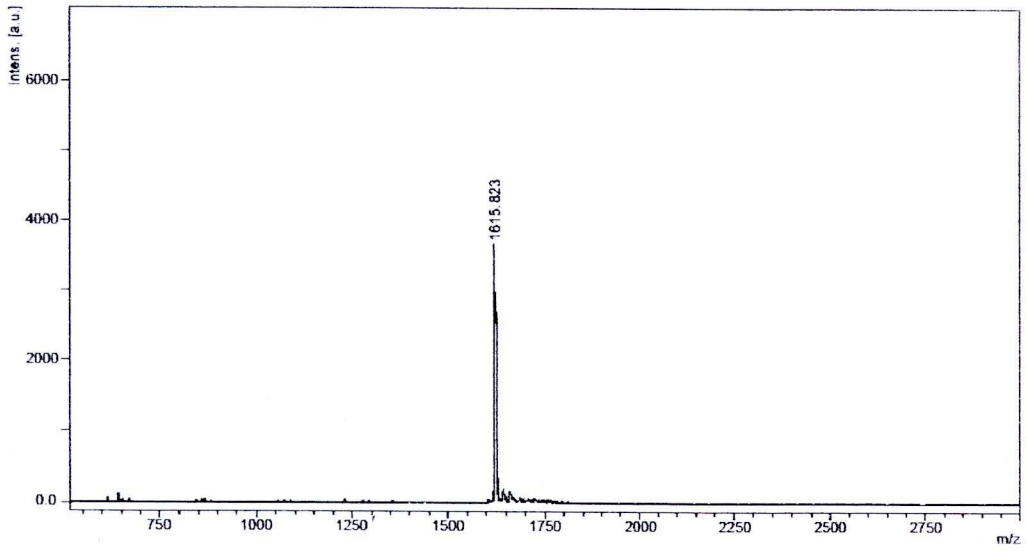

Figure 81 MALDI-TOF mass spectrum of purified NH_2-TTTTTT-$COONH_2$ (56c)

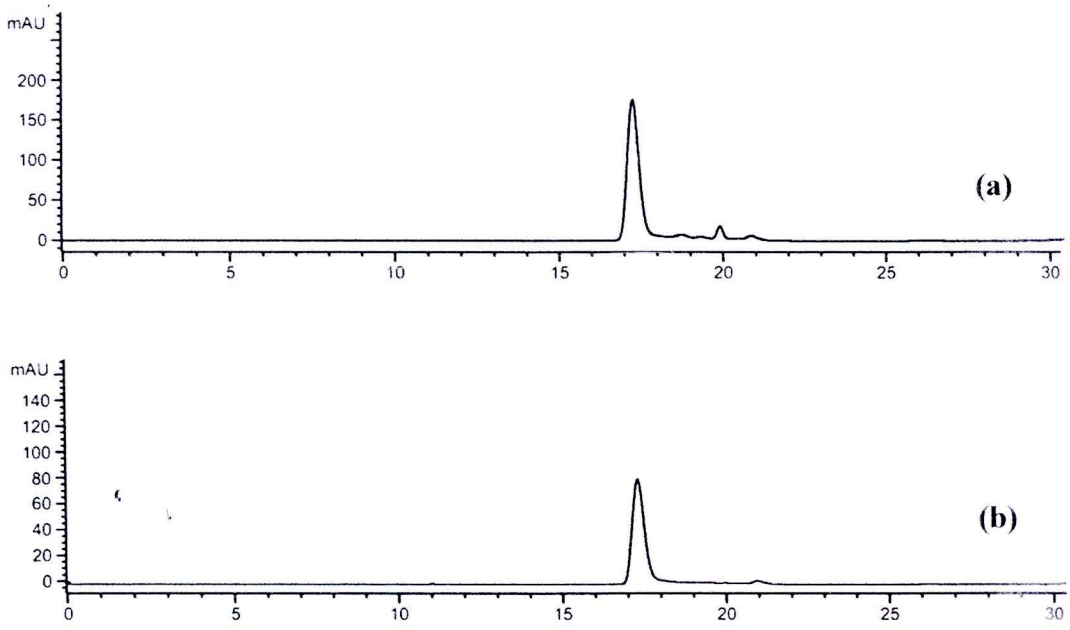

Figure 82 HPLC chromatogram of (a) crude and (b) purified NH_2-CBZ TTTTT-$COONH_2$ (56d)

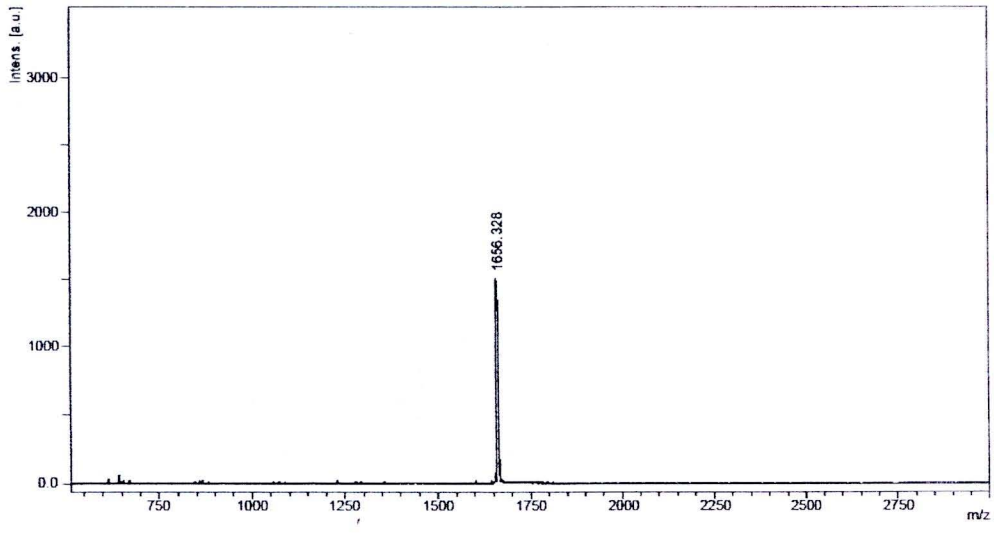

Figure 83 MALDI-TOF mass spectrum of purified NH_2-CBZ TTTTT-$COONH_2$ (56d)

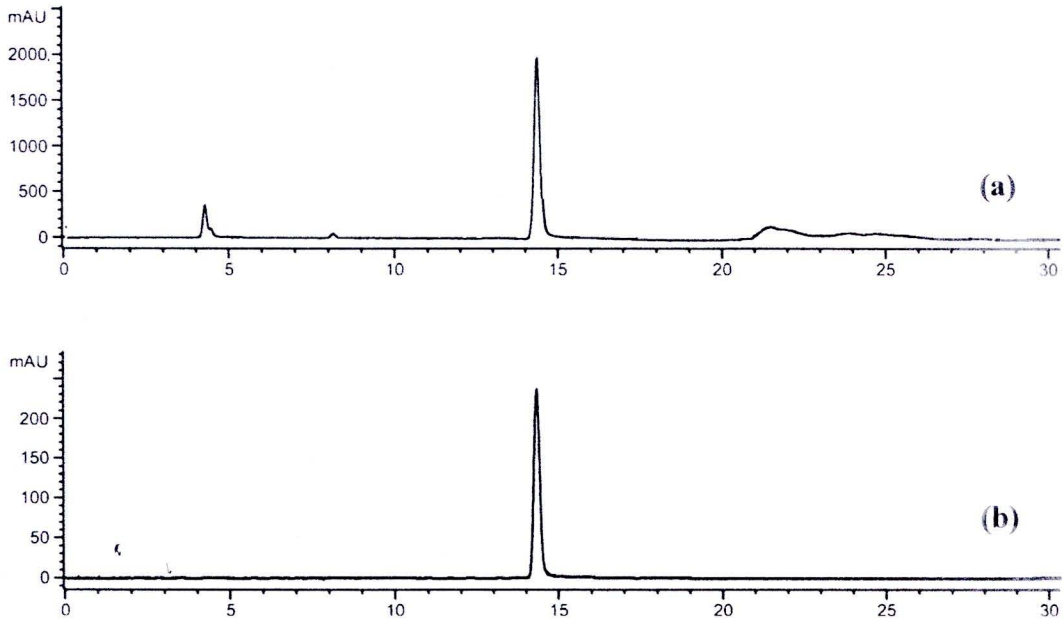

Figure 84 HPLC chromatogram of (a) crude and (b) purified NH_2-DCCBZ TTTTT-$COONH_2$ (56e)

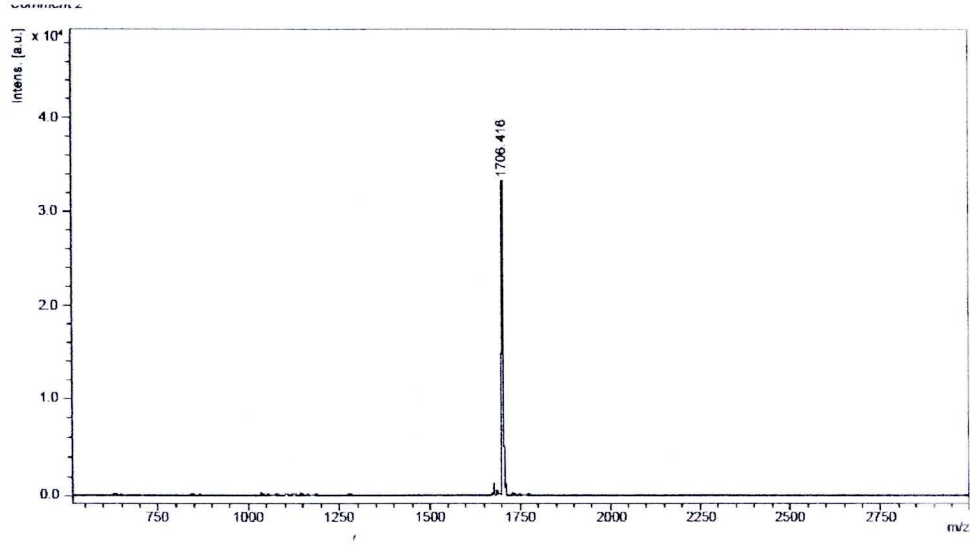

Figure 85 MALDI-TOF mass spectrum of purified NH_2-DCCBZ TTTTT-$COONH_2$ (56e)

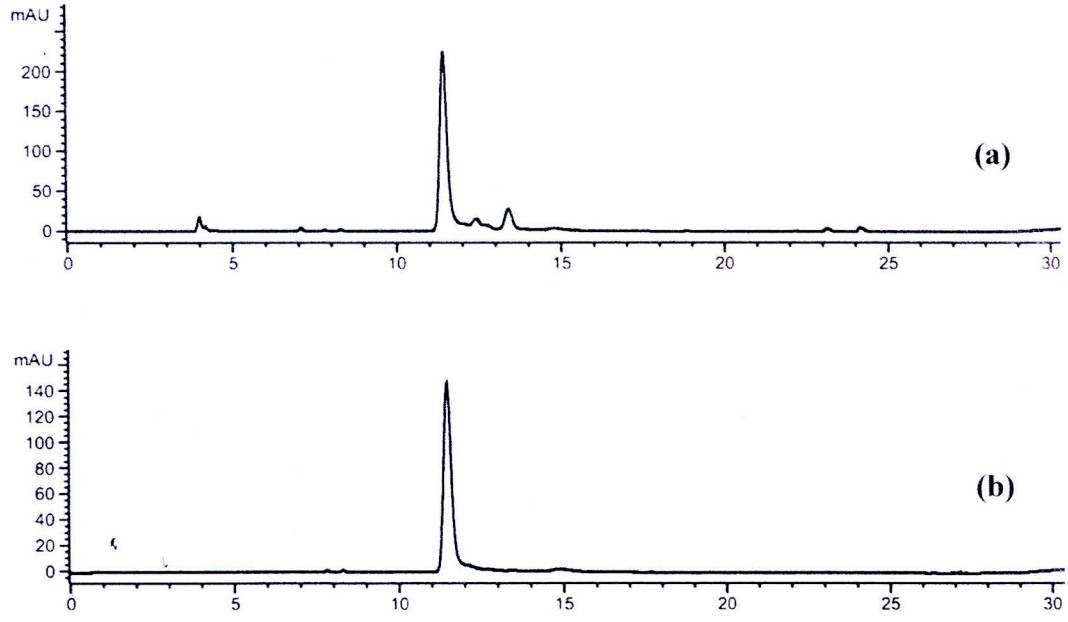

Figure 86 HPLC chromatogram of (a) crude and (b) purified NH_2-DNCBZ TTTTT-$COONH_2$ (56f)

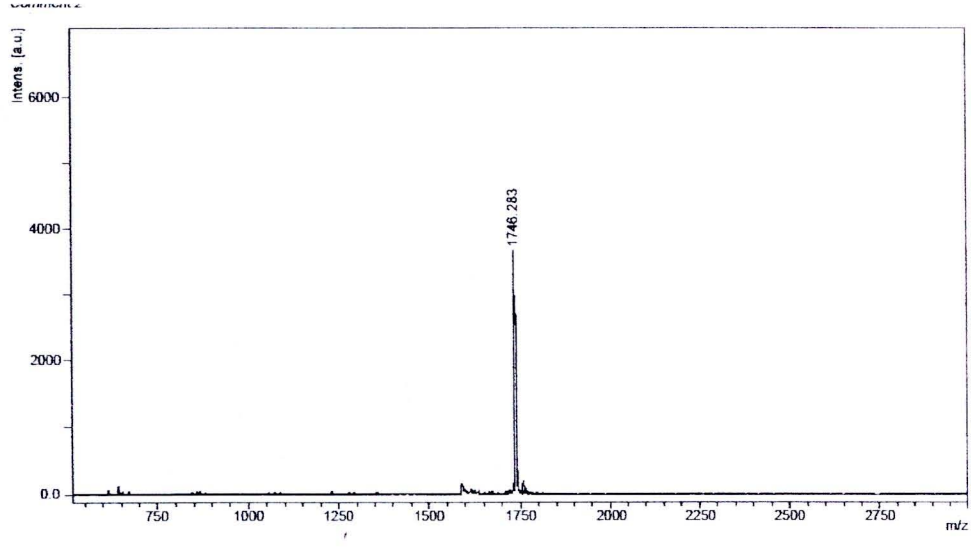

Figure 87 MALDI-TOF mass spectrum of purified NH_2-DNCBZ TTTTT-$COONH_2$ (56f)

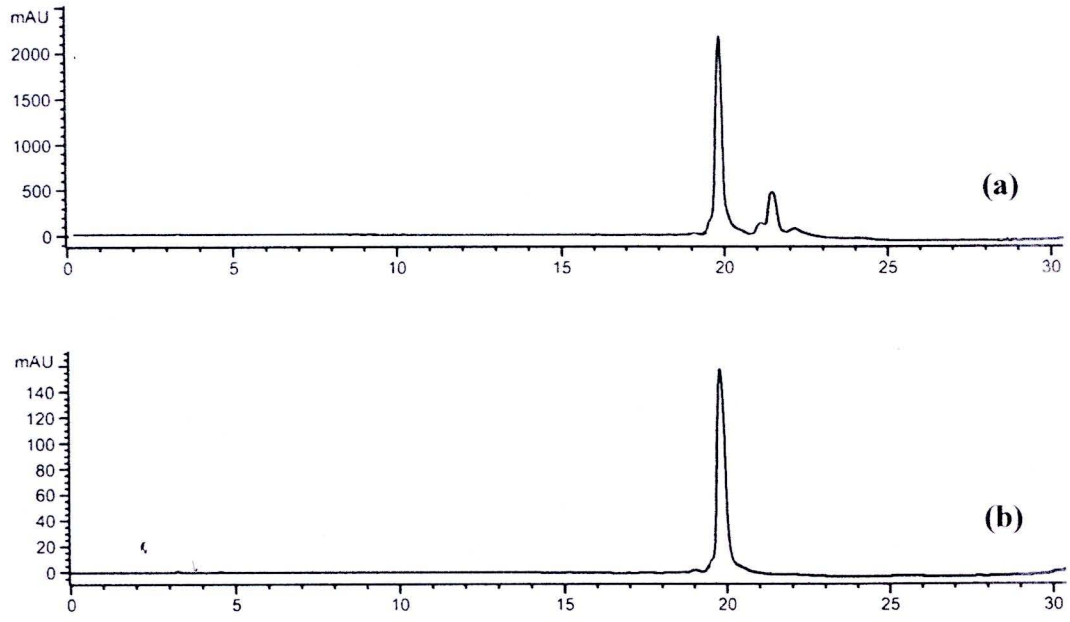

Figure 88 HPLC chromatogram of (a) crude and (b) purified NH_2-TTTTTTTT-$COONH_2$ (56g)

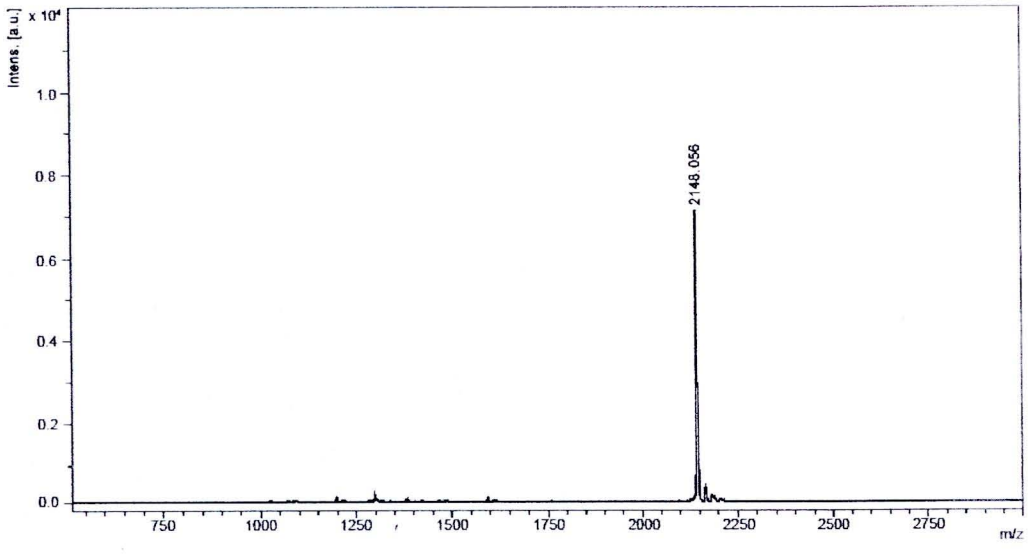

Figure 89 MALDI-TOF mass spectrum of purified NH_2-TTTTTTTT-$COONH_2$ (56g)

APPENDIX B : Synthesis of NH_2-*aeg*PNA-thymine-COOH and study of reactivity of 2-vinyl-4,4-dimethyl-5-oxazolone (VDM)

Synthesis of methyl 2-(2-(*tert*-butoxycarbonylamino)ethylamino)acetate (62) [89]

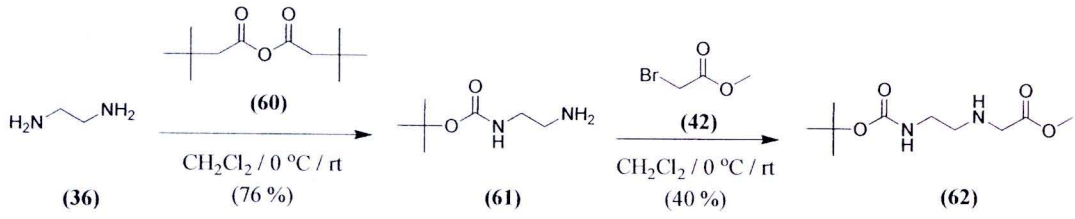

(36) (61) (62)

Scheme 35 Synthesis of methyl 2-(2-(*tert*-butoxycarbonylamino) ethylamino)acetate (62)

To a solution of ethylenediamine **(36)** (9.60 mL, 159.1 mmol) in anhydrous CH_2Cl_2 (30 mL) cooled in an ice bath, was added dropwise over period of 5 h. to a solution of di-*tert*-butyldicarbonate **(60)** (4.43 g, 20.29 mmol) in anhydrous CH_2Cl_2 (20 mL). After stirring overnight, the reaction mixture was washed with water (5 x 120 mL), dried over anhydrous Na_2SO_4, concentrated, and dried *in vacuo* to give crude product of *tert*-butyl 2-aminoethylcarbamate **(61)** as an oil. Without further purification, **61** (1.8 g, 11.23 mmol) was dissolved in anhydrous CH_2Cl_2 (30 mL), and diisopropylethylamine (DIEA) (1.95 mL, 11.79 mmol) was added. Then, a solution of methyl broacetate **(42)** (1.06 g, 11.79 mmol) was added dropwise over 1 h. The resulting solution was stirred at room temperature approximately 18 h. and washed with brine (5 x 30 mL). The organic layer was dried over anhydrous Na_2SO_4, filtered and and dried *in vacuo* to produce of **62** as a white solid in 40 % yield for two steps.

^{1}H NMR 400 MHz ($CDCl_3$) δ 4.87 (br, 1H, NH), 3.74 (s, 3H, CH_3), 3.60 (s, 2H, CH_2), 3.20 (t, 2H, CH_2, J= 6.3 Hz), 2.89 (t, 2H, CH_2, J=6.2 Hz), 1.85 (br, 1H, NH) 1.35 (s, 9H, $C(CH_3)_3$)

Synthesis of Boc-*aeg*PNA-thymine-methyl ester monomer (63) [89]

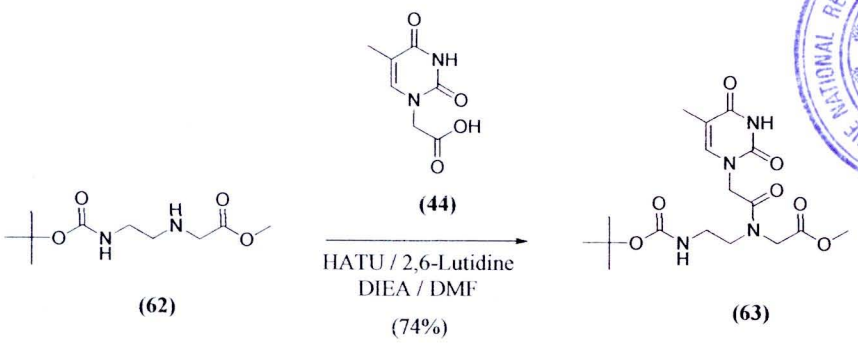

Scheme 36 Synthesis of Boc-*aeg*PNA-thymine-methyl ester monomer (63)

To a solution of **62** (0.50 g, 2.30 mmol) in anhydrous DMF (5 mL), was added DIEA (0.59 mL, 4.6 mmol), thymine-1-ylacetic acid **(44)** (0.51 g, 2.76 mmol), HATU (1.67 g, 4.42 mmol), and 2,6-lutidine (0.95 mL, 8.28 mmol). The reaction mixture was stirred for 8 h. at room temperature and then concentrated *in vacuo*. The residue was brought up in CH_2Cl_2 and washed with saturated $NaHCO_3$ (5 x 30 mL) and brine (5 x 15 mL). The organic layer was dried over anhydrous Na_2SO_4 and concentrated *in vacuo*. The crude product was purified by column chromatography (19:1 CH_2Cl_2/MeOH). The desired product **(63)** was obtained as a white solid in 74 % yield: R_f= 0.45 (9:1 CH_2Cl_2/MeOH)

^{1}H NMR 400 MHz ($CDCl_3$) δ 8.51 (br, 1H, NH), 6.97/6.83 (rotamer s, 1H, Ar), 5.63/5.38 (rotamer br, lH, NH), 4.53/4.38 (rotamer s 2H, CH_2), 4.21/4.10 (rotamer s, 2H, CH_2), 3.76 (s, 3H, CH_3), 3.49 (t, 2H, CH_2, J=6.4 Hz), 1.86/1.85 (rotamer s, 3H, CH_3), 1.64/1.46 (rotamer s, 9H, $C(CH_3)_3$)

Synthesis of Boc-*aeg*PNA-thymine-COOH (64)

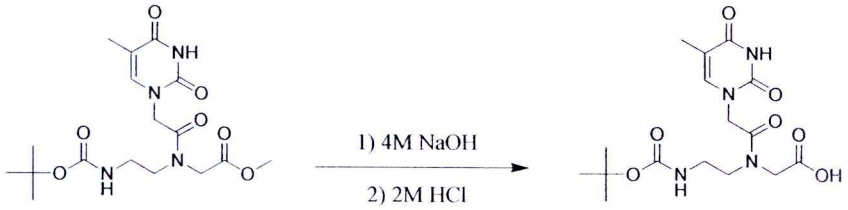

(63) (64)

Scheme 37 Synthesis of Boc-*aeg*PNA-thymine-COOH (64)

A suspension of **63** in 4 M NaOH was stirred for 45 min at room temperature. The reaction mixture was cooled to 0 ℃ and pH was adjusted to 2 with 2 N HCl. The aqueous solution was extracted with ethyl acetate (3 x 30 mL). The organic layer was dried over anhydrous Na_2SO_4 and concentrated *in vacuo*. The desired product **(64)** was obtained as a white solid in 79 % yield.

^{1}H NMR 400 MHz ($CDCl_3$) δ 8.87 (br, 1H, NH), 6.97/6.83 (rotamer s, 1H, Ar), 5.62/5.38 (rotamer br, lH, NH), 4.54/4.38 (rotamer s 2H, CH_2), 4.20/4.10 (rotamer s, 2H, CH_2), 3.49 (t, 2H, CH_2, J=6.3 Hz), 1.83/1.84 (rotamer s, 3H, CH_3), 1.63/1.48 (rotamer s, 9H, $C(CH_3)$)

Synthesis of NH_2-*aeg*PNA-thymine-COOH (65)

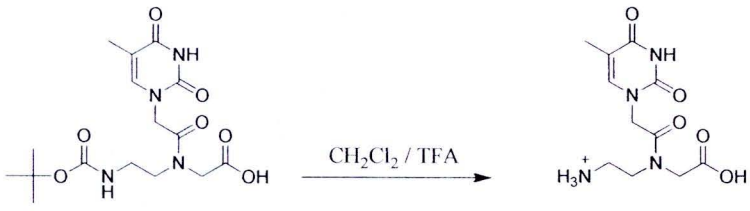

(64) (65)

Scheme 38 Synthesis of NH_2-*aeg*PNA-thymine-COOH (65)

A portion of desired Boc-*aeg*PNA methyl ester monomer **(64)** (200 mg) was treated with a 2:1 (V/V) mixture of TFA:CH_2Cl_2 (2 mL). The reaction mixture was stirred at the room temperature for 3 h. and was co-evaporated with toluene. The resulting crude product was dried *in vacuo* to remove TFA. The crude oil was washed with diethyl ether and dried *in vacuo.* The desired product **(65)** was obtained as a white-yellow solid in 74 % yield.

^{1}H NMR 400 MHz ($CDCl_3$) δ 8.85 (br, 1H, NH), 6.96/6.84 (rotamer s, 1H, Ar), 4.53/4.37 (rotamer s 2H, CH_2), 4.23/4.12 (rotamer s, 2H, CH_2), 3.50 (t, 2H, CH_2, J=6.2 Hz), 3.13(s, 2H, CH_2), 1.75 (s, 3H, CH_3)

Reactivity of amine and hydroxyl groups of *aeg*PNA with VDM

To a solution of **65**, VDM in anhydrous DMF (5 mL) was added. The reaction mixture was stirred at room temperature for 8 h. Then, the reaction mixture was concentrated *in vacuo* to give **66** as mastic solid and reaction were followed up by ^{1}H-NMR 400 Hz as shown in figure 90.

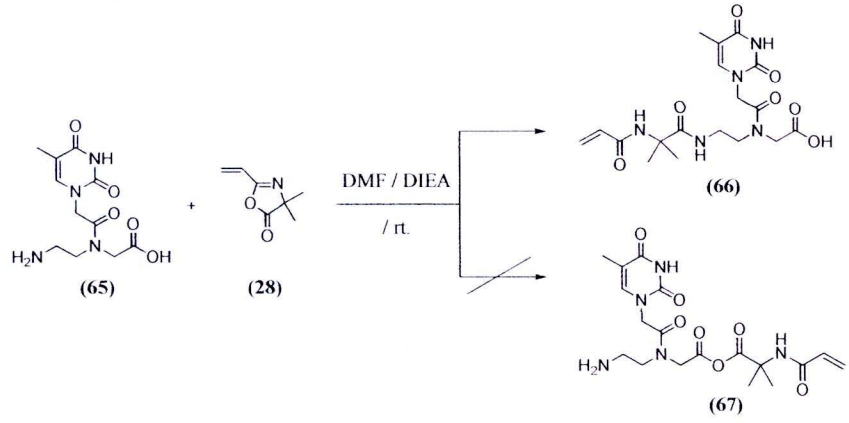

Scheme 39 Reactivity of amine and hydroxyl groups

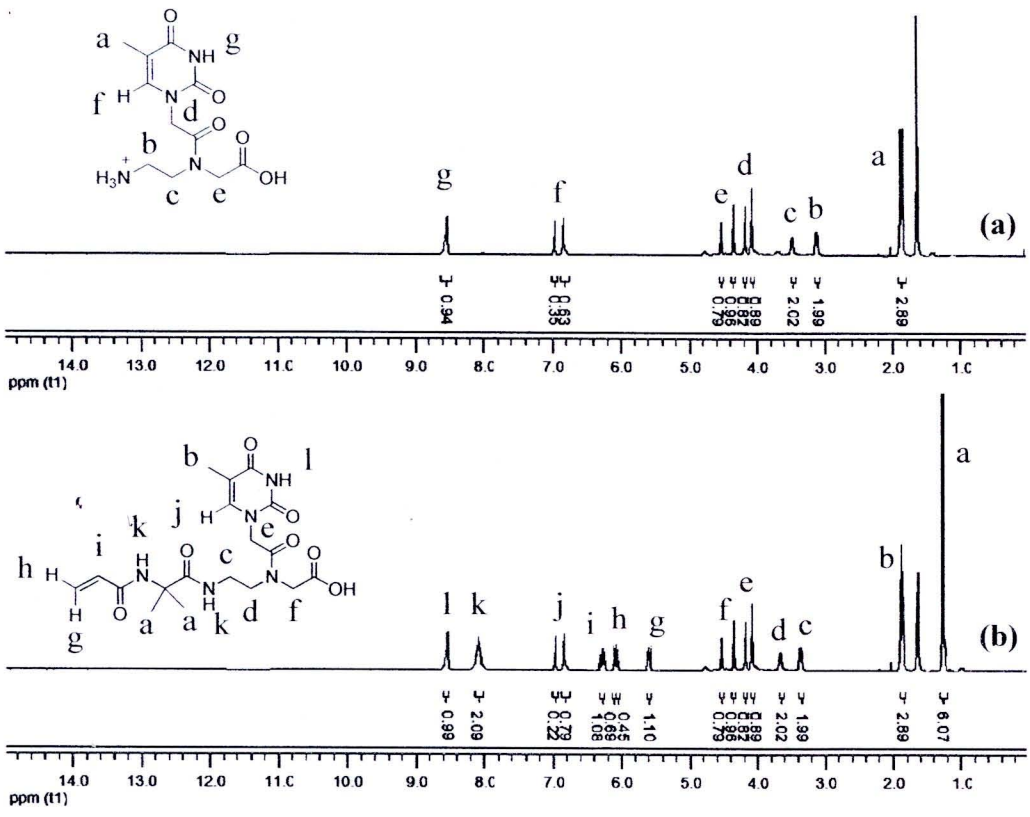

Figure 90 ^{1}H-NMR spectrum of (a) NH_2-*aeg*-thymine-COOH (65), (b) Product of reaction (66) ($CDCl_3$)

Optimization of VDM with hydroxyl groups of Boc-*aeg*PNA-T-COOH

To a solution of **64** and VDM (29) (Table 8) in anhydrous DMF (5 mL)was added. The reaction mixture was stirred at room temperature for 8 h. Then, the reaction mixture was concentrated *in vacuo* to give crude product as white solid and was followed up by ^{1}H-NMR 400 Hz as shown in figure 91.

Table 8 Mol eq. between Boc-*aeg*PNA-thymine-COOH and VDM

mol eq. ratio	
Boc-*aeg*PNA-T-COOH	**VDM**
1	1
1	2
1	4
1	6

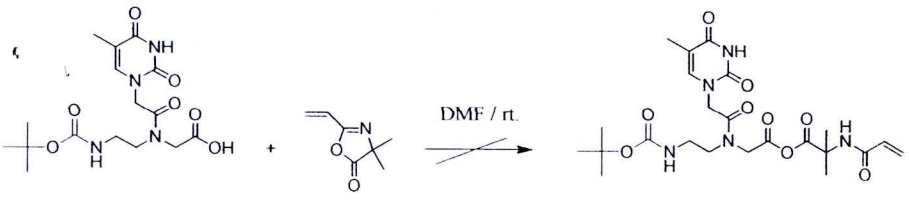

(64) (28) (68)

Scheme 40 Optimization of VDM with hydroxyl groups

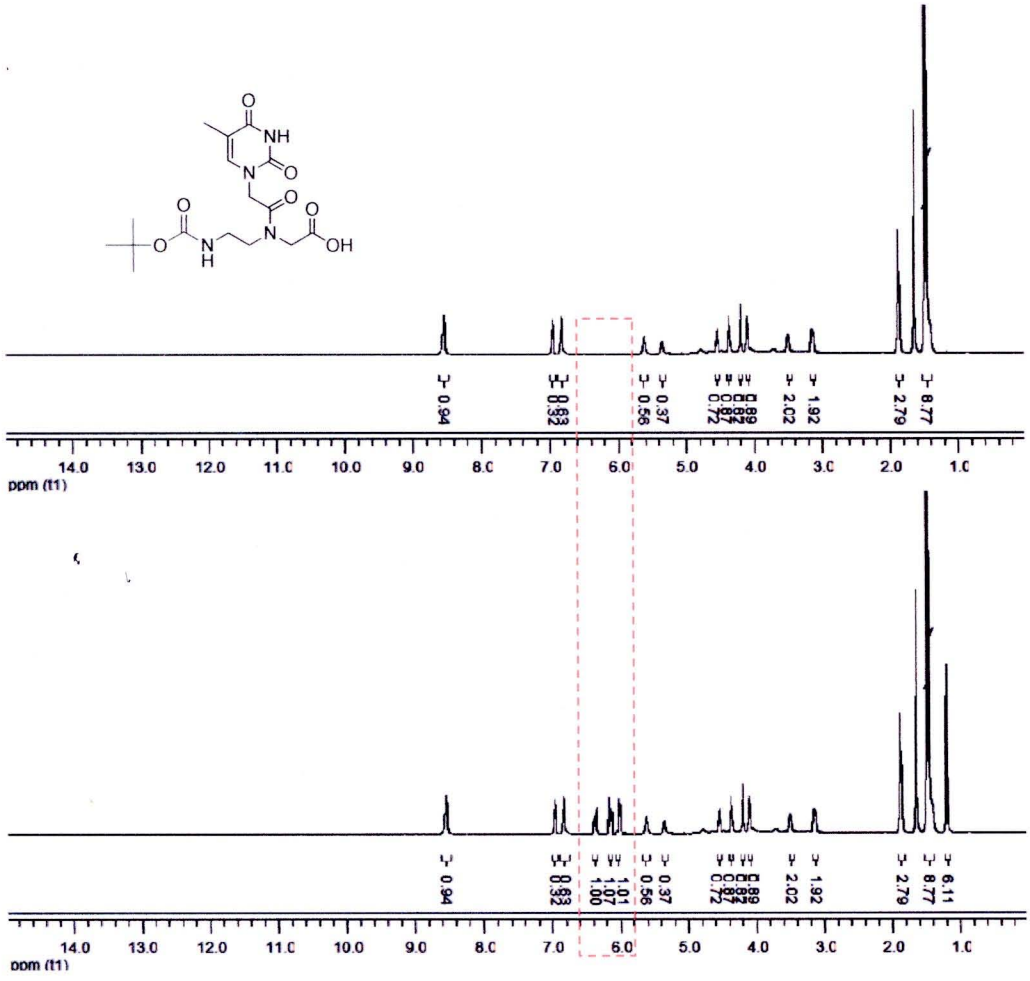

Figure 91 ^{1}H-NMR spectrum of (a) Boc-*aeg*PNA thymine COOH (64) (b) Product of reaction retio 1:6 ($CDCl_3$)

APPENDIX C : Extinction coefficient of carbazole derivative acetic acid and coupling efficiency of each monomer

Determination of extinction coefficient of carbazole derivatives

Stock solutions of *aeg*PNA oligomers in water were quantitated by measuring the absorbance at 260 nm using the following values for the extinction coefficients of individual residues for PNA, A=13,700, C=6,600, G=11,700, and T=8,600 $l.mol^{-1}cm^{-1}$. The extinction coefficients for carbazole derivative were obtained from the experiment as described.

A stock solution approximately ~10 mM of carbazole derivatives in 100 mL of 100 mM $NaHCO_3$ was prepared. Next, the stock solutions were diluted with 100 mM $NaHCO_3$ to give three different concentrations (for example: 0.01 mM, 0.02 mM, and 0.03 mM). Then, each diluted solution was heated at 55 °C for at least 1 minute. The absorbance of the solution was then measured at 260 nm. The average of the three absorbance measurement was used to calculate the extinction coefficients using Beer's law (eq : 4):

$$A = \varepsilon bc \qquad (4)$$

Where: A = absorbance

ε = extinction coefficient ($l.mol^{-1}.cm^{-1}$)

b = path length of the cell (cm)

c = concentration of the solution ($mol.l^{-1}$)

Extinction coefficient was determined from three concentrations. The three extinction coefficients were averaged, and this averaged value was used in the quantitation of PNA oligomer concentrations.

Table 9 Extinction coefficient of carbazole derivative

Compounds	Extinction coefficient ($l.mol^{-1}.cm^{-1}$)
carbazole acetic acid (**42**)	18,239
3,6- dicyanocarbazole acetic acid (**48**)	20,283
3,6- dinitrocarbazole acetic acid (**50**)	18,533

The coupling efficiency of each monomer

To check the effectiveness of each coupling step, the solution consists of dibenzofulvene and 20 % piperidine in anhydrous DMF was measured with UV-vis spectrometry at 290 nm. The first absorbance of the solution from the first loading of Fmoc-*aeg*PNA-resin, was assumed to be 100%. The efficiency should be up to 95 % for each step in order to give acceptable yield.

The *aeg*PNA oligomer was synthesized according to protocol using MBHA-resin (10 mg, 1.0 μmol). The coupling efficiency of each monomer was shown in the table C1.

Table 10 The coupling efficiency of each monomer

Code	Cycle	Monomers	A_{290}	Coupling efficiency (%)
T_2				
	1	Fmoc-*aeg*PNA-T-COOH	0.813	100.00
	2	Fmoc-*aeg*PNA-T-COOH	0.775	95.39
	Average			97.69

Table 10 (cont.)

Code	Cycle	Monomers	A_{290}	Coupling efficiency (%)
T_4				
	1	Fmoc-*aeg*PNA-T-COOH	0.801	100.00
	2	Fmoc-*aeg*PNA-T-COOH	0.784	97.88
	3	Fmoc-*aeg*PNA-T-COOH	0.772	98.51
	4	Fmoc-*aeg*PNA-T-COOH	0.756	97.89
	Average			98.57
T_6				
	1	Fmoc-*aeg*PNA-T-COOH	0.816	100.00
	2	Fmoc-*aeg*PNA-T-COOH	0.786	96.37
	3	Fmoc-*aeg*PNA-T-COOH	0.753	95.80
	4	Fmoc-*aeg*PNA-T-COOH	0.724	96.15
	5	Fmoc-*aeg*PNA-T-COOH	0.689	95.17
	6	Fmoc-*aeg*PNA-T-COOH	0.648	93.96
	Average			96.24
TC_6				
	1	Fmoc-*aeg*PNA-T-COOH	0.890	100.00
	2	Fmoc-*aeg*PNA-T-COOH	0.873	98.05
	3	Fmoc-*aeg*PNA-T-COOH	0.850	97.40
	4	Fmoc-*aeg*PNA-T-COOH	0.828	97.37
	5	Fmoc-*aeg*PNA-T-COOH	0.797	96.22
	6	Fmoc-*aeg*PNA-C-COOH	0.763	95.73
	Average			97.46

Table 10 (cont.)

Code	Cycle	Monomers	A_{290}	Coupling efficiency (%)
TCC_6				
	1	Fmoc-*aeg*PNA-T-COOH	0.810	100.00
	2	Fmoc-*aeg*PNA-T-COOH	0.800	98.77
	3	Fmoc-*aeg*PNA-T-COOH	0.783	97.83
	4	Fmoc-*aeg*PNA-T-COOH	0.759	96.89
	5	Fmoc-*aeg*PNA-T-COOH	0.740	97.58
	6	Fmoc-*aeg*PNA-DCC-COOH	0.703	95.00
	Average			97.68
TNC_6				
	1	Fmoc-*aeg*PNA-T-COOH	0.783	100.00
	2	Fmoc-*aeg*PNA-T-COOH	0.771	98.47
	3	Fmoc-*aeg*PNA-T-COOH	0.757	98.23
	4	Fmoc-*aeg*PNA-T-COOH	0.741	97.89
	5	Fmoc-*aeg*PNA-T-COOH	0.708	95.50
	6	Fmoc-*aeg*PNA-DNC-COOH	0.586	82.81
	Average			95.48
T_8				
	1	Fmoc-*aeg*PNA-T-COOH	0.838	100.00
	2	Fmoc-*aeg*PNA-T-COOH	0.820	97.85
	3	Fmoc-*aeg*PNA-T-COOH	0.795	96.95
	4	Fmoc-*aeg*PNA-T-COOH	0.775	97.40
	5	Fmoc-*aeg*PNA-T-COOH	0.744	96.04
	6	Fmoc-*aeg*PNA-T-COOH	0.707	94.98
	7	Fmoc-*aeg*PNA-T-COOH	0.681	96.42
	8	Fmoc-*aeg*PNA-T-COOH	0.651	95.60
	Average			96.91

APPENDIX D : Limit of detection (LOD) and Limit of Quantitation (LOQ) calculation

Limit of detection (LOD) and Limit of Quantitation (LOQ) calculation by Miller method

Table 11 Absorption, SD and %RSD of thymine *aeg*PNA monomer at 5, 10, 30, 50 and 100 µM

Conc.	Abs					Average	SD	%RSD
5	0.0461	0.0457	0.0445	0.0450	0.0447	0.0452	0.0006	1.41
10	0.0830	0.0839	0.0856	0.0843	0.0851	0.0844	0.0010	1.14
30	0.2540	0.2647	0.2528	0.2612	0.2668	0.2599	0.0059	2.28
50	0.4523	0.4407	0.4242	0.4417	0.4390	0.4396	0.0095	2.16
100	0.8547	0.8482	0.8422	0.8582	0.8591	0.8525	0.0068	0.79

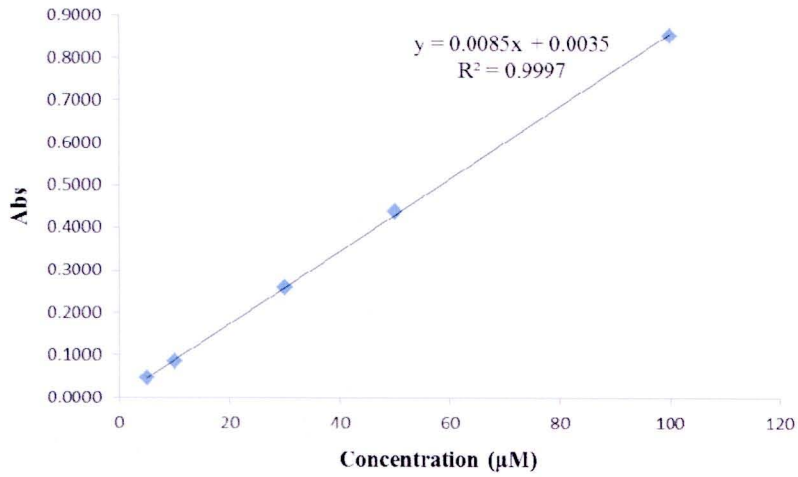

Figure 92 Calibration curve of NH_2-*aeg*-thymine-COOH (60) at 10, 30, 50 and 100 µM

Limit of detection (LOD)

$$y_{LOD} = y_B + 3s_B \quad (5)$$

Limit of quantitative (LOQ)

$$y_{LOQ} = y_B + 10s_B \quad (6)$$

when; y_{LOD} = Signal generated for LOD

y_{LOQ} = Signal generated for LOQ

y_B = y-Intercept of equation

s_B = Standard deviation of blank

Form

$$y = 0.0085x + 0.0035 \quad (7)$$

y_B = 0.0035

when; x = Concentration of *aeg*PNA thymine monomer

y = Absorption of *aeg*PNA thymine monomer

y_i = Absorption of *aeg*PNA thymine monomer by $y = 0.0085x + 0.0035$

$$s_B = \sqrt{\frac{\sum (y - yi)^2}{N - 2}}$$

Table 12 Calculation of detection limit

x (μM)	y	y_i	$y-y_i$	$(y-y_i)^2$
5	0.0452	0.0460	-0.0008	0.00000064
10	0.0844	0.0885	-0.0041	0.00001697
30	0.2599	0.2585	0.0014	0.00000196
50	0.4396	0.4285	0.0111	0.00012277
100	0.8525	0.8535	-0.0010	0.00000104
			$\sum(y-yi)^2$	0.00014
			$\sum(y-yi)^2/N-2$	0.00005
			s_B	0.00691
			y_B	0.00350
			$y_{LOD} = y_B + 3s_B$	2.44
			$y_{LOD} = y_B + 10s_B$	8.12

BIOGRAPHY

BIOGRAPHY

Name-Surname Kritsada Tankanya

Date of Birth February 21, 1987

Address 229 Moo 5, Sankhong, Amphoe Dok-kham-tai, Phayao, Thailand. 56120

Education Background

2008 B.S. (Chemistry) Naresuan University, Phitsanulok, Thailand